



Motion compensation of a K-type installation vessel using suction piles

Konstantinos Kiskiras

Motion compensation of a K-type installation vessel using suction piles

by

Konstantinos Kiskiras

in partial fulfillment of the requirements for the degree of

Master of Science

at the Delft University of Technology,
to be defended publicly on Monday October 2, 2017.

Thesis Committee:	Prof. dr. A.V. Metrikine,	TU Delft
	Ir. C. Keijdener,	TU Delft
	Dr. F. Pisanò,	TU Delft
	Ir. K. van der Heiden,	Jumbo Shipping

An electronic version of this thesis is available at <http://repository.tudelft.nl/>.



Acknowledgements

This report is the result of the research I conducted at Jumbo Maritime for the master degree in Off-shore & Dredging Engineering at Delft University of Technology. In order to complete this study, I received support from many people. I would like to thank every person that helped me during this graduation thesis.

First of all I would like to thank you Jumbo for giving me the opportunity of executing this project. Working at Jumbo has been a great experience during the last nine months. I would especially like to thank my supervisor from Jumbo, Kasper van der Heiden, for his support and his advice. I am very happy for our cooperation during the whole period of my graduation study.

I would also like to thank, my daily supervisor in TU Delft, Chris Kijdener, for his suggestions. They were quite important for the completion of this project. Moreover, I would like to thank the chairman of my graduation committee Prof. Andrei Metrikine, for his guidance during this study.

Furthermore, I want to thank my friends in Greece and in Delft for their encouragement, patience and support. Lastly, I would like to thank my family for their constant support all these years. Their love and encouragement helped me to finish this graduation study.

Konstantinos Kiskiras

Delft, October 2017

Abstract

Jumbo is a heavy lift, shipping, offshore transportation and installation contractor. Jumbo has been an experienced company in ocean transportation for more than 45 years. Since 2003, building on their heavy lift capability, Jumbo is rapidly getting involved in the offshore installation market.

Jumbo normally uses dynamic positioning systems for the stabilization of the vessels during the installation process. These systems are quite expensive and there is a need for alternative options for the stabilization of the vessels. One idea is the use of spudpoles for a K-type installation vessel which are inserted into the soil and connected to the vessel via hydraulic cylinders. The spudpoles transfer the loads caused by the motions of the vessel to the soil resulting in the reduction of the movements of the vessel. The goal of this project is the reduction of the motions of the vessel in offshore operation improving its workability. A design of the compensation system along with an investigation of its performance are necessary in order to achieve this.

A survey of several types of foundation for the spudpoles is conducted in order to find the appropriate solution for this specific project. After a Multi Criteria Analysis the suction bucket solution was selected since it is a quick and easy way to for the penetration and extraction of the piles, at the start and the end of the installation procedure respectively.

To model the vessel, a 6 degrees of freedom (DOF) time domain model was created. The hydrodynamic coefficients as well as the response amplitude operators (RAO) were obtained with the diffraction program WAMIT. For the calculation of the motions of the vessel the time consuming convolution integral was replaced by an extensive state space system. This specific model was validated using a Matlab model based on the convolution scheme. The two spudpoles were discretized using finite differences. Moreover, for a better representation of a real life situation, an irregular sea state was used. In the final state space model, the vessel, the spudpoles, the hydraulic cylinders and the environmental loads are included.

Steel type S355 was selected for the initial design of the spudpoles. After performing the necessary stress and buckling checks for the spudpoles and taking into consideration the limitations of the motions of the vessel, it came out that the required thickness of the spudpoles was too large and so the type of steel was changed to S690. A number of simulations were performed with several sets of different diameter and thickness in order to obtain the optimum design. Furthermore, the suction buckets were checked for their pull-out and bearing capacity. A final design was selected for both the spudpoles and the suction buckets taking into account the outcome of the checks and the limitations of the vessel's motions. The vessel moves between the allowable limits for the 6 DOF, proving that this compensation system is a realistic and feasible solution.

Based on the performed simulations, the critical wave directions were identified. The wave directions of 105° and 135° are the two critical for the stress and buckling checks. The wave direction of 90° is the critical one for the pull-out capacity check of the suction buckets. These wave directions should be avoided during the operation to assure higher safety standards for the vessel.

Contents

1	Introduction	1
1.1	Problem description	1
1.2	Thesis objective	1
1.3	Research approach and outline	1
1.4	Motion definitions	2
1.5	Wave heading conventions	4
2	Foundation selection	5
2.1	Spudpoles with a conical end	5
2.1.1	Advantages	5
2.1.2	Disadvantages	6
2.2	Monopiles with vibrating hammer	6
2.2.1	Advantages	6
2.2.2	Disadvantages	7
2.3	Suction piles	7
2.3.1	Advantages	8
2.3.2	Disadvantages	8
2.3.3	General remarks	9
2.4	Multi Criteria Analysis	9
3	The vessel model	11
3.1	Equation of motion	11
3.1.1	Equation of motion in frequency domain	11
3.1.2	Equation of motion in time domain	11
3.1.3	Selection of the appropriate domain	12
3.2	Software selection	12
3.3	Degrees of freedom	12
3.4	Hydrodynamic and Hydrostatic coefficients	13
3.4.1	Hydrodynamic coefficients	13
3.4.2	Conversion of the added mass and damping coefficients from WAMIT	13
3.4.3	Extension of the hydrodynamic coefficients	14
3.4.4	Hydrostatic coefficients	15
3.5	Creating the model	15
3.5.1	State space system	15
3.5.2	Creating a Single Input Single Output Model	16
3.5.3	Creating a Multi Input Multi Output Model	19
3.6	Model validation	20
3.6.1	Check the model's stability	20
3.6.2	Comparison between 2 Matlab models	21
4	Compensation system	23
4.1	Hydraulic cylinders	23
4.2	Hydraulic stiffness of the system	23
4.3	Configuration of the system	24
4.4	Location of the compensation system	24
4.5	Installation process	25
5	Wave Loads	29
5.1	Wave Loading on the vessel	29
5.1.1	Regular waves	29



5.1.2	Irregular waves	29
5.1.3	Dispersion relationship	30
5.1.4	Response amplitude operator (RAO)	30
5.1.5	Wave spectrum	31
5.1.6	Diffraction force	33
5.2	Wave Loading on the spudpoles	34
5.2.1	Wave potential and water particle velocity	34
5.2.2	Wave and current velocity	35
5.2.3	Morison equation	37
5.2.4	Implementation of the acceleration term in the Morison equation	37
6	Modelling of the spudpoles	39
6.1	Implementation of the spudpoles	39
6.2	Connection with the state space model of the vessel	40
6.3	The lower part of the spudpoles	41
7	Checks	43
7.1	Checks for the spudpoles	43
7.1.1	Stress check	44
7.1.2	Global buckling check	44
7.2	Checks for the suction bucket	46
7.2.1	Pull-out capacity check	46
7.2.2	Bearing capacity check	47
8	Results	49
8.1	Simulation for the initial design	49
8.1.1	Motions of the vessel	49
8.1.2	Motion of the spudpoles	50
8.1.3	Checks	51
8.2	Extra tests for optimization	52
8.3	The optimum design	53
8.3.1	Motion of the vessel	53
8.3.2	Motion of the spudpoles	54
8.3.3	Final Checks	54
9	Conclusions and Recommendations	57
9.1	Summary	57
9.2	Results Analysis	57
9.3	Recommendations	58
9.4	Contributions of this project	58
	Appendices	61
	Appendix A JUMBO KINETIC Specifications	61
	Appendix B Finite differences scheme	62
	Appendix C Motions of the vessel	64
	Appendix D Motions of the spudpoles	69

List of Figures

1.1	Structure of the report	2
1.2	The six degrees of freedom of the vessel.	3
1.3	Side View of the Jumbo Kinetic vessel.	3
1.4	Top view of the Jumbo Kinetic vessel.	4
1.5	Definition of wave headings.	4
2.1	Spud lifting systems.	5
2.2	Vibrating hammer.	6
2.3	Installation process of a suction pile.	8
3.1	A-values from WAMIT and extended A-values.	14
3.2	B-values from WAMIT and extended B-values.	15
3.3	Transfer functions of the 36 elements.	17
3.4	Comparison between real and approximate program.	18
3.5	Motions of the vessel after applying initial conditions.	20
3.6	Comparison of the results of the two models.	21
4.1	Double acting hydraulic cylinder.	23
4.2	Compensation System.	24
4.3	Location of the compensation systems.	25
4.4	The compensation systems.	25
4.5	The sailing phase.	26
4.6	The upending phase.	26
4.7	The lowering phase.	27
4.8	The penetration phase.	27
5.1	The superposition principle.	30
5.2	RAO for roll motion.	31
5.3	JONSWAP spectrum.	31
5.4	Error as a function of frequency components.	32
5.5	Discretized wave spectrum with 43 components.	33
5.6	Discretized wave spectrum with 170 components.	33
5.7	Water velocity profile as a function of z/d	35
5.8	Total water velocity profile as a function of z/d	36
5.9	Water acceleration profile as a function of z/d	36
6.1	Comparison between FD scheme and analytical solution results.	40
6.2	Rotation around the three axes.	41
6.3	Suction bucket dimensions.	42
7.1	Characteristics of a circular hollow section.	43
7.2	The variation of minimum yield strength with thickness.	43
7.3	Buckling length coefficient.	44
7.4	Buckling curves a-d.	45
7.5	External and internal friction forces.	46
8.1	The 6 motions of the vessel for a simulation of 400sec ($D=8m$ and $t=0.4m$).	50
8.2	The motions of the spudpoles in x and y direction for a simulation of 400sec ($D=8m$ and $t=0.4m$).	51
8.3	Critical wave directions.	52
8.4	Test results.	53
8.5	The 6 motion of the vessel for 400sec simulation ($D=11m$ and $t=0.10m$).	53
8.6	The motions of the spudpoles in x and y direction for a simulation of 400sec ($D=11m$ and $t=0.10m$).	54
8.7	The 6 motions of the vessel for a simulation of 400sec ($D=11m$ and $t=0.10m$).	55



8.8	The motions of the spudpoles in x and y direction for a simulation of 400sec (D=11m and t=0.10m).	55
B.1	Discretization of a beam	62
C.1	The 6 motion of the vessel (D=8m,t=0.35m,Wave direction 105°).	64
C.2	The 6 motion of the vessel (D=8m,t=0.40m,Wave direction 105°).	64
C.3	The 6 motion of the vessel (D=8m,t=0.40m,Wave direction 135°).	65
C.4	The 6 motion of the vessel (D=9m,t=0.30m,Wave direction 105°).	65
C.5	The 6 motion of the vessel (D=9.5m,t=0.09m,Wave direction 105°).	66
C.6	The 6 motion of the vessel (D=10m,t=0.09m,Wave direction 105°).	66
C.7	The 6 motion of the vessel (D=10m,t=0.25m,Wave direction 105°).	66
C.8	The 6 motion of the vessel (D=11m,t=0.09m,Wave direction 105°).	67
C.9	The 6 motion of the vessel (D=11m,t=0.10m,Wave direction 105°).	67
C.10	The 6 motion of the vessel (D=11m,t=0.10m,Wave direction 90°).	68
D.1	The motions of the spudpoles in x and y direction (D=8m,t=0.35m,Wave direction 105°).	69
D.2	The motions of the spudpoles in x and y direction (D=8m,t=0.40m,Wave direction 105°).	69
D.3	The motions of the spudpoles in x and y direction (D=8m,t=0.40m,Wave direction 135°).	70
D.4	The motions of the spudpoles in x and y direction (D=9m,t=0.30m,Wave direction 105°).	70
D.5	The motions of the spudpoles in x and y direction (D=9.5m,t=0.09m,Wave direction 105°).	70
D.6	The motions of the spudpoles in x and y direction (D=10m,t=0.09m,Wave direction 105°).	71
D.7	The motions of the spudpoles in x and y direction (D=10m,t=0.25m,Wave direction 105°).	71
D.8	The motions of the spudpoles in x and y direction (D=11m,t=0.09m,Wave direction 105°).	72
D.9	The motions of the spudpoles in x and y direction (D=11m,t=0.10m,Wave direction 105°).	72
D.10	The motions of the spudpoles in x and y direction (D=11m,t=0.10m,Wave direction 90°).	73

List of Tables

2.1	Calculation/ Estimation of weight factors.	9
2.2	The score for the three alternatives.	9
4.1	Area definition.	25
8.1	Maximum values of the 6 motions of the vessel.	50
8.2	Maximum values of the displacement of the spudpoles.	51
8.3	Maximum values of the checks.	51
8.4	Test parameters and results for steel type S355.	52
8.5	Test parameters and results for steel type S690.	52
8.6	Maximum values of the 6 motions of the vessel.	54
8.7	Maximum values of the displacement of the spudpoles.	54
8.8	Maximum values of the checks.	56

1 Introduction

1.1 Problem description

Jumbo is a heavy lift shipping, offshore transportation and installation contractor. Jumbo has been an experienced company in ocean transportation for more than 45 years. Since 2003, building on their heavy lift capability, Jumbo is rapidly getting involved in the offshore installation market.

At the same time, there is a big boost of the offshore wind energy. It is a relatively new renewable energy source with a limited impact on the environment and on humans. Another advantage is the fact that this type of energy has no limits since the wind will always blow. On the other hand this benefit causes a lot of problems. There are no limits because it is a renewable form of energy but there are limitations in several fields such as construction, installation and transportation. New opportunities have arisen during the last years and the support structures of the wind turbines are getting bigger. It follows that the installation and the transportation become more difficult since extra accuracy is needed.

Regarding the installation, which will be an essential point of this project the main issue is the motion of the vessels. When the vessels are located in the harbor, they are quite safe without any extreme environmental loads on them but in the open sea (e.g. North Sea) the situation is totally different. There are a lot of factors that influence the motion of the vessel such as waves, current, wind, moving fluid in tanks and also the load distribution on the deck. The motions are quite larger and they affect the procedure of the installation. During the installation of a transition piece for example, a possible crash between the transition piece and the monopile will likely cause damage on the substructure.

There are two ways in order to eliminate this negative effect. The first one is the installation during specific weather windows and the second is the reduction of the motions of the vessel. Regarding the first way, the vessel should be in operation only specific periods of the year (when the weather is good and there are not large environmental loads) resulting in a limited workability. This method is insufficient and also causes losses for the company, concerning both reputation and financial loss. For the second way there are several projects aiming to the reduction of the motion of the vessels (see section 1.4). In this project a motion compensation system will be examined in order to check if it is a reliable method in order to reduce the motions and increase the workability of the vessel. This motion compensation system consists of two spudpoles, which will be attached on the vessel with the use of hydraulic cylinders and they will be inserted in the soil. An analytical description and a visualization of the system can be found in section 4.3.

1.2 Thesis objective

With the problem description mentioned, the following research objective of this thesis can be summarized in the following point:

The goal of this project is the reduction of the motions of an installation vessel (Jumbo K-type) in offshore operation improving its workability. In order to achieve this, a design of the compensation system and an investigation of its performance for several sea states are needed.

1.3 Research approach and outline

An overview of this project is presented in Figure 1.1. Each one of the blocks represents a main part of the project. Each arrow shows the direction of the general procedure and the double arrows represent an iteration procedure. The number of the chapter, in which each part of the thesis can be found, is shown in the block as well.

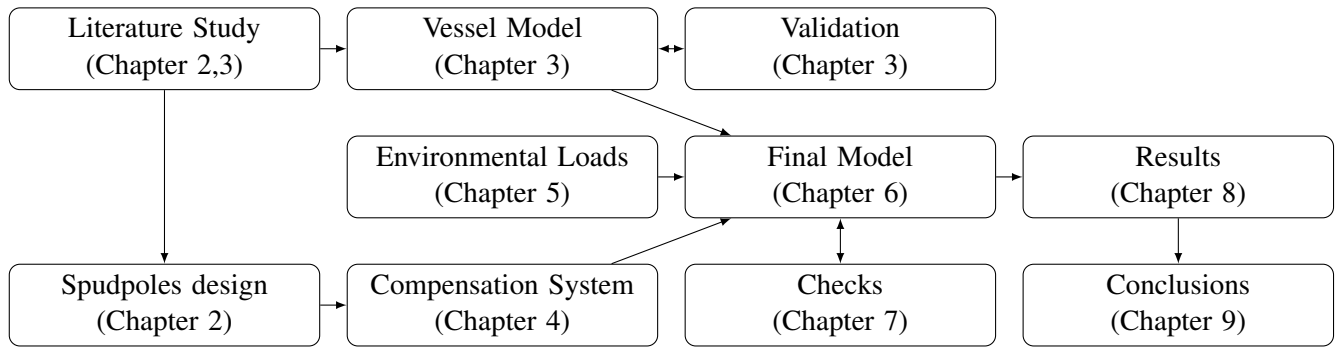


Figure 1.1: Structure of the report

In the introduction (Chapter 1) the problem and the objective of this project are described. Also some useful definitions are given. The research about the spudpoles and the comparison between them are described in Chapter 2. In Chapter 3, a time domain model of the Jumbo K-type vessel is created. In order to avoid issues with non-linearities a time domain model is used, so all the coefficients should be transferred from frequency to time domain. In the same chapter, there is a validation of the model in order to make sure that the initial model will work properly. The definition of the compensation system and the role of the hydraulic cylinders on it are presented in Chapter 4. The whole process of the calculation of the environmental loads on both the vessel and the spudpoles is displayed in Chapter 5. To continue with, the construction of the spudpoles model based on the Euler-Bernoulli beam is described in Chapter 6. The next step is the combination of the three models (Vessel, Environmental loads and compensation system) to one general model in Chapter 6. Based on a procedure of iterations the optimum design will be found (Chapter 7) and the results are presented in the following (Chapter 8). The conclusions and the recommendations of this project will be discussed in the last chapter. Finally, in the appendices some extra information about the vessel and analytical derivations can be found.

1.4 Motion definitions

The vessel, like every floating object, can move in six degrees of freedom. Three of them are translations and the other three are rotations. For x, y and z coordinate system around the center of gravity of the vessel the motions can be defined as follows. The three translations are:

Surge: motion in the X direction

Sway: motion in the Y direction

Heave: motion in the Z direction

And the three rotations are:

Roll: rotation around X axis (ϕ)

Pitch: rotation around Y axis (θ)

Yaw: rotation around Z axis (ψ)

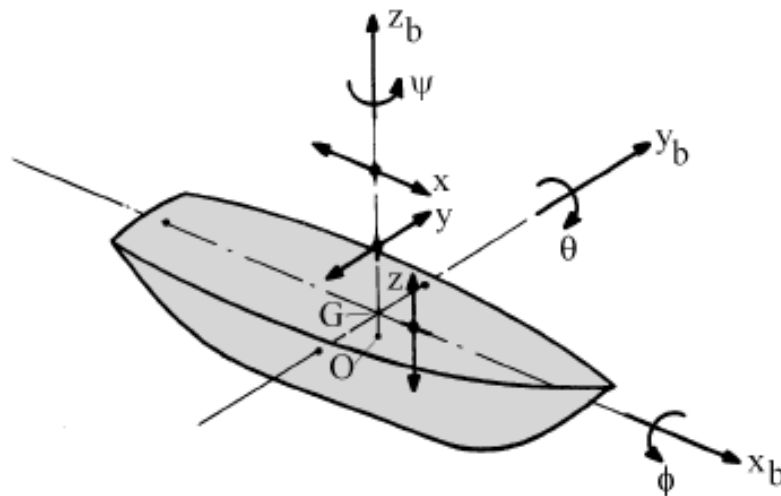


Figure 1.2: The six degrees of freedom of the vessel.

The definitions of the axis system are presented in the Figure 1.2. It should be noted that the center of gravity is not the same point with the center of rotation. The vessel in reality rotates around the center of rotation. This point is in the middle of the vessel as regards the y axis but it is in the middle of the distance of the two cranes of the vessel regarding the x -axis. The z coordinate of the center of rotation is the deck height of the vessel minus the metacenter height. The general arrangement of the vessel, as well as the position of the center of rotation, can be observed in the following Figures.

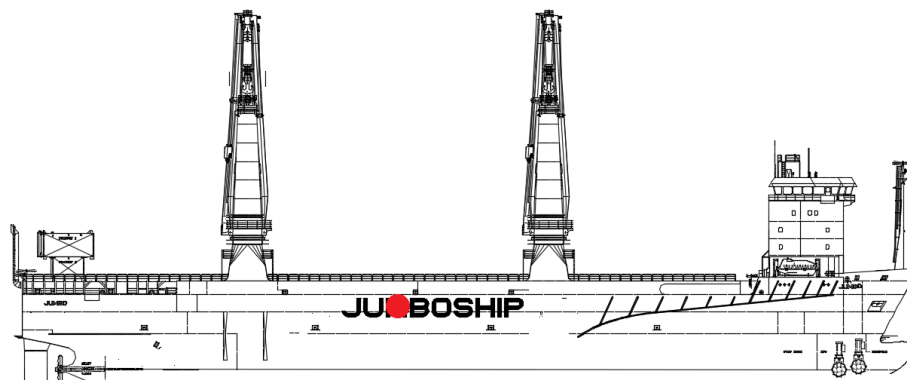


Figure 1.3: Side View of the Jumbo Kinetic vessel.

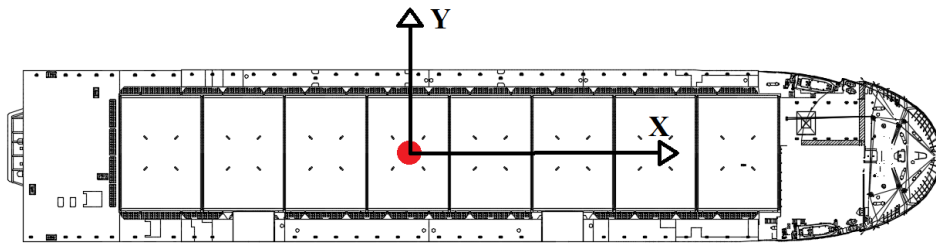


Figure 1.4: Top view of the Jumbo Kinetic vessel.

The center of rotation is indicated by the red dot.

1.5 Wave heading conventions

The waves can be characterized by their direction based on the direction of the vessel. The waves, which have the same direction with the vessel are called stern waves (heading of 0°). On the other side, the waves of the opposite side are called bow waves (heading of 180°). Waves coming from both portside (heading of 90°) and starboard (heading of 270°) are called beam waves. This wave heading convention is presented in Figure 1.5.

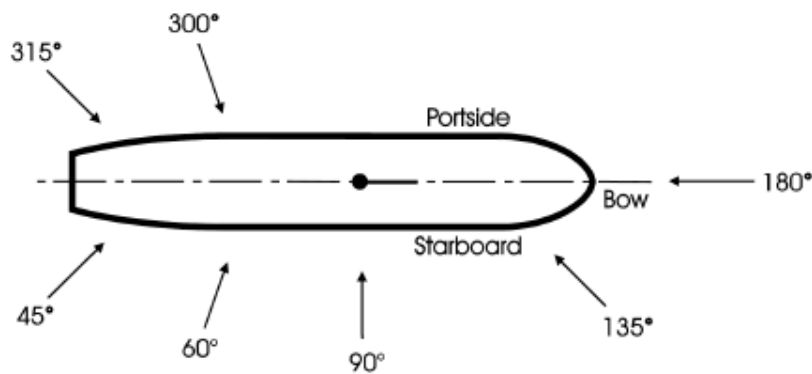


Figure 1.5: Definition of wave headings.

2 Foundation selection

The general concept of this project is the reduction of the motion of the vessel with the use of spudpoles. The spudpoles will be inserted into the soil in order to transfer the loads from the vessel to the soil. There are several types of foundation of the spudpoles based on former experience from cutter suction dredger vessels and wind turbine foundations. Each one has advantages and at the same time drawbacks for this special type of construction. In the following chapter an analysis of the foundation types is given. Firstly there is an analysis of three foundation types presenting the advantages and disadvantages of each one and then a MCA (Multi Criteria Analysis) is made in order to select the most appropriate type for the specific case of the Jumbo vessel. The examined foundation types are the following:

- spudpoles with a conical end
- monopile
- suction piles

2.1 Spudpoles with a conical end

Spudpoles with a conical end are mainly used in dredging industry and especially in the cutter suction dredgers for stabilization of the vessel during the operation. The lowering of the poles is made by their self weight of the poles and by the help of wires, winches or spud hoist cylinders. The spud lifting system for the spudpoles is based on the three following possible mechanisms [1]:

- The spud is hoisted by means of a wire attached to the upper end.
- The spud can be hoisted on a wire that runs through a pulley mounted on the underside of the spud.
- The spud is hoisted by an extending cylinder. The spud hoist cylinders have a specific stroke of approximately 2-4 m.

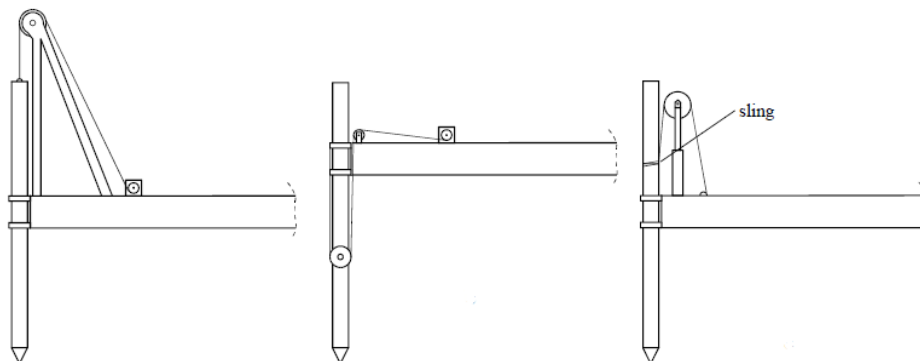


Figure 2.1: Spud lifting systems.

2.1.1 Advantages

The advantages of the use of the spudpoles are :

- With the presence of a lifting and lowering winch the pole will be pushed in addition to its own weight into the ground.
- The spud poles can move up and down at own convenience and fast.
- There is no need for extra cranes.
- They are used widely in the dredging industry, so there is previous experience.

2.1.2 Disadvantages

On the other hand, the disadvantages of the spudpoles are:

- It is an expensive solution as the lifting and lowering winch costs about 150000 € per pole. There is also some extra maintenance cost as the steel cable (4-5 cm diameter) should be replaced every year. And this will cost about 3750 € per year per pole [2].
- Furthermore an extra hydraulic powerpack is needed. This costs around 60000 €. So there is additional cost [2].
- Spudpoles have a small range of diameters. Up to 2.2 m e.g. the spud system of the vessel Athena. This diameter is quite small and it will probably be a limitation for the specific design of this project.
- Lastly, the holding capacity of the spuds depend on the soil conditions in the specified area.

2.2 Monopiles with vibrating hammer

Another alternative for the foundation of the poles of the vessel is the use of monopiles (the same with the offshore wind industry) in combination with hammers. As it is described in the previous section there is a need of a way for an easy penetration as well as extraction of the pile, since the vessel will change location after the installation. So for this reason the conventional hammers are not useful because they cannot be used in the extraction. On the other hand, the vibrating hammers are suitable for the penetration and extraction of the monopiles from the soil. The vibrations reduce the friction between the soil and the pile, thus allowing a fast and easy penetration. The main advantages and disadvantages of this alternative follow on the following sections [3].



Figure 2.2: Vibrating hammer.

2.2.1 Advantages

The advantages of the monopile in combination with the use of a vibrating hammer are:

- The main advantage of vibrating hammers in comparison with the classic hydraulic hammers is that they can be used for the extraction of the pile from the soil.

- It also reduces the damage to marine life (in a radius of 2 km instead of 20 km with the hammering). They also produce less noise (less decibels).
- The vibratory piling is up to ten times faster and quieter compared to impact hammering (the duration of the vibration plus jetting is about one hour including the load-bearing capacity certificate instead of 10 hours, for a steel pile with 3.5 m diameter, 60 m length and insertion depth of 24m. The duration of the pre-vibrating and post-hammering procedure is about 5 hours).
- Another advantage is that the vibrating hammer will be used for a more accurate position of the pile. There is a possibility of correction of the misplacement errors, because they have the possibility to correct the angle of the pile during insertion procedure.
- They can also handle large diameter monopiles.
- Furthermore the hammer moves horizontally stored piles into the vertical positions.

2.2.2 Disadvantages

The disadvantages of this method are:

- A disadvantage of the vibrating hammer is that it cannot vibrate dense, hard soils (e.g. rock). The solution for those hard soils is the combination of vibrating and hammering of the pile.
- Also one crane should lift the hammer for the vibration procedure.
- Moreover the purchase of a vibrating hammer is imperative.

2.3 Suction piles

Suction pile is a hybrid design between a gravity base foundation and a monopile combining the benefits of both. The bucket foundation depending on the skirt length and diameter can have a bearing capacity similar to that of a monopile, a gravity foundation or in between. Suction piles seem to be quite competitive in the range of 20-55 m water depth. The installation process is as follow:

- The suction pump unit is attached to the foundation.
- The foundation is lowered to the seabed.
- Dead-weight and gravity ensures self-penetration into the seabed.
- The pump unit enables under-pressure inside the bucket and a water-jet alongside the skirt tip ensure local seabed liquefaction. This combination ensures soil penetration.
- Verticality is controlled to reach required inclination tolerance
- The suction pump unit is recovered.

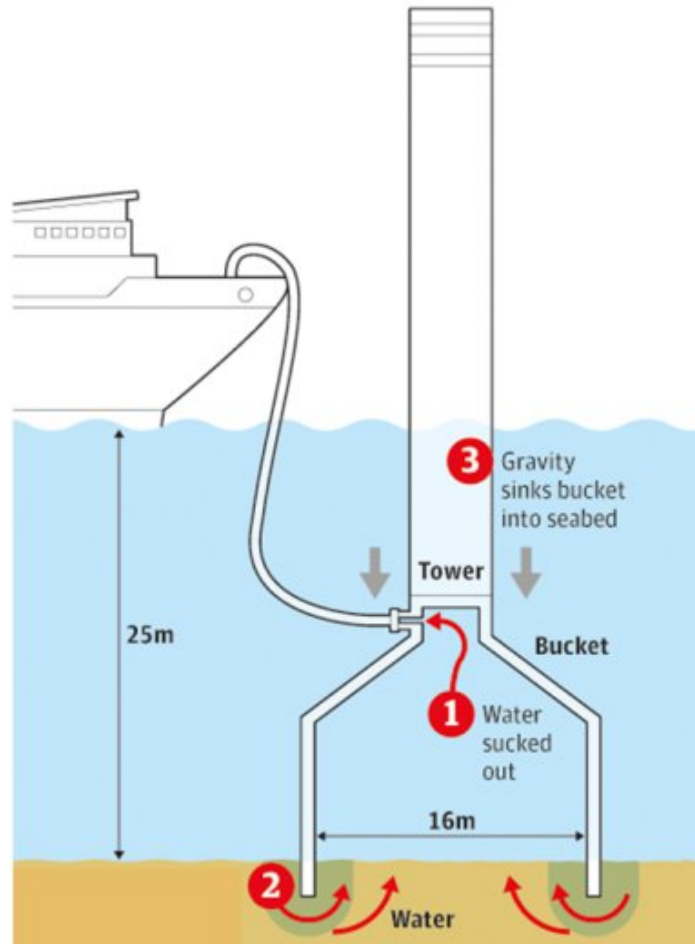


Figure 2.3: Installation process of a suction pile.

The process of the installation of a suction bucket can be visualized in Figure 6.3.

2.3.1 Advantages

The advantages of this relatively new method are the following:

- For the construction of a suction pile it is used 25% less steel than for the comparable monopile, so it is a cost-effective solution.
- There is no need for any seabed preparations.
- In addition to the installation is noise free and it offers no risk to marine mammals.
- The suction operation can be reversed allowing the complete removal of foundations and the re-use of them in the next location.
- Lastly the installation is quicker. The whole process is faster as there is no need for hammering.

2.3.2 Disadvantages

The disadvantages of this foundation type are:

- Suitable for a specific range of soils. They cannot be used in all soil types rather are only applicable in sand and clay of intermediate strength. This fact makes them unsuitable for harder soil types and increases the risks during installation.

- They are thin shell structures, as the ratio between the bucket diameter and wall thickness is very large. Buckling is therefore a major design consideration.
- Furthermore for high loads, for example in case of large water depths, monopiles are to be preferred in order to achieve the required limitation of deformations of the foundation construction.
- Liquefaction is the phenomenon when soil loses its strength and stiffness. This can be crucial for suction caissons and there is not a lot supporting the structure and a failure of soil will result in the failure of the support.
- It is a complicated structure and it requires extensive welding work.

2.3.3 General remarks

Suction piles provide a greater resistance to vertical and lateral loads than driven piles due to their larger diameters. Their main loading issue is overturning moment. Regarding the penetration velocity, the value is now around 2m/hour but there is room for optimization during the following years.

2.4 Multi Criteria Analysis

To assess the three alternative foundation types, several criteria were taken into account, in which a weight factor of importance is given. In order to calculate the weight factors for every parameter, values based on their significance are given in each one of them. In the following Table, only values of 0, 0.5 and 1 were chosen. In each cell, if the parameter in the row is more important than the parameter in the column, then the value 1 is used, and consequently if it is less important the value 0 is used. If both parameters are considered to be of equal importance, then the value 0.5 is used. The cells that correspond to the same parameters in row and columns (diagonal cells) have value of 1. In the last column the weight factor is calculated by adding up the values in the row and divide the sum with the total number of the parameters.

	Insertion	Extraction	Installation time	Fabrication cost	Operation cost	Noise level	Weight factor
Insertion	1	0.5	0.5	1	0.5	0.5	0.72
Extraction	0.5	1	0.5	1	0.5	0.5	0.72
Installation time	0.5	0.5	1	0.5	0.5	1	0.64
Fabrication Cost	0	0	0.5	1	0.5	0.5	0.36
Operation Cost	0.5	0.5	0.5	0.5	1	1	0.72
Noise level	0.5	0	0	0.5	0	1	0.36

Table 2.1: Calculation/ Estimation of weight factors.

Then, the three selected foundation types are being evaluated based on a scale from 1 to 10, where 10 is the most favorable on the different criteria. Based on this evaluation the final score is calculated.

	Insertion	Extraction	Installation time	Fabrication cost	Operation cost	Noise level	Score
Spudpoles	5	7	6	6	5	8	21.0
Monopile	6	6	8	6	6	6	22.3
Suction piles	7	7	5	7	7	7	23.3

Table 2.2: The score for the three alternatives.



From the above analysis, it becomes clear that the suction piles would definitely be the most suitable choice for the foundation of the vessel. The major advantage of the suction buckets is the fact that they can be inserted into the soil and be extracted from it easily in comparison with the other two alternatives. The concept of this project is the installation of transition pieces of wind turbines so a quick way for stabilization of the vessel in different locations is required. These locations will be mostly in the North Sea, where the main type of soil is sand. So the suction buckets are quite suitable for this type of soil. The disadvantage of the complex design is a strong drawback, but since only two piles will be constructed, the total cost will not be so high. If this design was for a wind farm with 80 or 100 foundations the total cost would be quite large and in this case this complex design should be taken carefully into consideration.

3 The vessel model

In the following section a model for the motions of the vessel will be presented. The construction of the model will be analyzed in simple steps. With the help of the model the motions of the vessel are calculated for several sea states and at a next level the two spudpoles will be inserted into the model. A worth mentioning point is that the scope of this project is not the construction of the perfect model (because of the limited time also) but the construction of a model which will describe in a quite accurate way the motions of the vessel with the presence of the two spudpoles.

3.1 Equation of motion

The equation of the motion for the vessel is based on the Newton's first law for both domains.

$$M_i \cdot \ddot{x}_i(t) = \sum F \quad (3.1)$$

On the left hand side of the equation 3.1 the accelerations are shown as the second time derivative of x_i (the displacement of the body), where the counter i represents the three deflections (surge, sway, heave for $i= 1,2,3$) and the three rotations (roll, pitch, yaw for $i= 4,5,6$) of the vessel. The M represents the mass of the vessel for the three first degrees of freedom of the vessel and the moment of inertia for the next three degrees of freedom. On the right hand side there is the summation of the applied forces on the vessel. This summation contains both the forces due to the motion of the vessel and the environmental forces.

3.1.1 Equation of motion in frequency domain

In the frequency domain the equation of motion of the vessel based on the equation 3.1 is the following:

$$(M + A(\omega)) \cdot \ddot{x} + B(\omega) \cdot \dot{x} + K \cdot x = F \quad (3.2)$$

Where:

M is the Mass Matrix (6 by 6)

A is the Added Mass Matrix (6 by 6)

B is the Damping Matrix (6 by 6)

K is the Stiffness Matrix (6 by 6)

F is the Force Vector (6 by 1)

ω is the Frequency range

Added mass is the inertia added to the system because an accelerating or decelerating body must move (or deflect) some volume of surrounding fluid as it moves through it. Added mass coefficients are proportional to the acceleration of the vessel. Damping coefficients in the damping matrix **B** shows the damping of the system in specific movements and they are proportional to the velocity of the vessel. The matrix **K** contains the hydrostatic restoring coefficients. The added mass and damping coefficients are frequency dependent. They are calculated with the use of the program WAMIT.

WAMIT is a radiation/diffraction panel program developed for the linear analysis of the interaction of surface waves with offshore structures. A major feature is the option to use a higher-order method based on B-splines to represent the velocity potential and pressure on the body surface in various manners. In addition to the conventional low-order panel discretization, these include new options to represent the body surface more accurately and/or with less work [4].

3.1.2 Equation of motion in time domain

According to the time domain approach which is analyzed in Offshore Hydromechanics [5] the equation of motion of the vessel in the time domain is the following:

$$(M + A) \cdot \ddot{x}(t) + \int_{-\infty}^t B(t - \tau) \cdot \dot{x}(\tau) \cdot d\tau + K \cdot x(t) = F(t) \quad (3.3)$$



where $B(t)$ and $B(\tau)$ are retardation functions and t, τ is time. By replacing τ by $t-\tau$ inside the integral the equation can be rewritten as:

$$(M + A) \cdot \ddot{x}(t) + \int_0^{\infty} B(\tau) \cdot \dot{x}(t - \tau) \cdot d\tau + K \cdot x(t) = F(t) \quad (3.4)$$

In the equation 3.4 the retardation function $B(\tau)$ is:

$$B(t) = \rho \iint_S \frac{\partial \chi(t - \tau)}{\partial t} \cdot n \cdot dS \quad (3.5)$$

and the added mass term is:

$$A = \rho \iint_S \Psi \cdot n \cdot dS \quad (3.6)$$

Where:

χ = normalized velocity potential cause by a displacement during time interval

\mathbf{n} = generalized directional cosine in a vector notation

Ψ = normalized velocity potential caused by a displacement during time interval

S = wetted surface

The velocity potentials, Ψ and χ , have to be found to determine the coefficients, A and B . A direct approach is rather complex [5]. Moreover, the convolution integral of the damping part in the equation 3.6 is quite hard to solve and also time consuming. For this reasons, the equation 3.16 will not be used but instead a general state space model will be used. This different approach will be analyzed later on this report.

3.1.3 Selection of the appropriate domain

Both frequency and time domain are accepted and used in the offshore industry. They also have advantages as well as disadvantages. The frequency domain is faster and not so time consuming for the calculations but it is more limited than time domain because it cannot be applied if there are non-linearities in the model. On the other hand time domain approach is more complicated and quite more time consuming than the frequency domain but it has the strong advantage of handling non-linearities in the model. If the construction of a model of the vessel was the only concern of this project the frequency domain would be the selected solution. But now in the model will be a combination of the vessel with the 2 spudpoles and maybe mooring lines (or something similar) so the time domain model will be selected in order to ensure that the model can also handle non-linearities.

3.2 Software selection

There is a big range of programs which can handle the simulation of the motions of a vessel like Orcaflex or Ansys Aqwa. On the other hand there is the solution of constructing the whole model in Matlab. Matlab is a well known and well used program in universities and research. There was an initial idea to make the model in Ansys Aqwa but it has no good interaction with Matlab scripts. Matlab is a necessity for some aspects of the thesis so it is decided to construct the whole model from the start in Matlab which is a user friendly and well known program and it is also strong in calculations and mathematics. Another drawback for Ansys Aqwa is that for the learning of this program a quite large amount of time is needed and this is not the purpose of this thesis.

3.3 Degrees of freedom

An important issue for the setup of the model is the number of the degrees of freedom which should be taken into account. The initial idea was to reduce the number of the 6 degrees of freedom to 3 in order

to examine one plane of the motions of the vessel. On the other hand the main concern of this project is the behavior of the vessel in all the degrees of freedom during the installation process. So despite the limited time of this project a selection of 6 degrees of freedom is chosen in order to achieve a better understanding of the reality and the optimum design of the spudpoles and the compensation system.

3.4 Hydrodynamic and Hydrostatic coefficients

3.4.1 Hydrodynamic coefficients

The mass matrix of the vessel is the following:

$$M = \begin{bmatrix} M & 0 & 0 & 0 & 0 & 0 \\ 0 & M & 0 & 0 & 0 & 0 \\ 0 & 0 & M & 0 & 0 & 0 \\ 0 & 0 & 0 & I_{xx} & 0 & I_{xz} \\ 0 & 0 & 0 & 0 & I_{yy} & 0 \\ 0 & 0 & 0 & I_{zx} & 0 & I_{zz} \end{bmatrix} \quad (3.7)$$

where M is the mass of the vessel with the cargo and the I is the inertia. It is assumed that the vessel has port-starboard symmetry so the $I_{xz}=I_{zx}=0$. In any case the roll-yaw inertia (so the yaw-roll inertia) are quite small in comparison with the other elements of the mass matrix and can be ignored. One more assumption is that the vessel has a fore-aft symmetry. Under this assumption the added mass and damping coefficients have the following form.

$$A = \begin{bmatrix} A_{11} & 0 & A_{13} & 0 & A_{15} & 0 \\ 0 & A_{22} & 0 & A_{24} & 0 & A_{26} \\ A_{31} & 0 & A_{33} & 0 & A_{35} & 0 \\ 0 & A_{42} & 0 & A_{44} & 0 & A_{46} \\ A_{51} & 0 & A_{53} & 0 & A_{55} & 0 \\ 0 & A_{62} & 0 & A_{64} & 0 & A_{66} \end{bmatrix} \quad (3.8)$$

$$B = \begin{bmatrix} B_{11} & 0 & B_{13} & 0 & B_{15} & 0 \\ 0 & B_{22} & 0 & B_{24} & 0 & B_{26} \\ B_{31} & 0 & B_{33} & 0 & B_{35} & 0 \\ 0 & B_{42} & 0 & B_{44} & 0 & B_{46} \\ B_{51} & 0 & B_{53} & 0 & B_{55} & 0 \\ 0 & B_{62} & 0 & B_{64} & 0 & B_{66} \end{bmatrix} \quad (3.9)$$

This assumption is proven correct by the results of the WAMIT. The values of the zero elements of the 2 above matrices are quite low and they can be ignored.

3.4.2 Conversion of the added mass and damping coefficients from WAMIT

Both added mass and damping coefficients provided from WAMIT are dimensionless. So they should be converted in SI units in order to be used in the equation of motion. The added mass coefficients (A_{ij}) should be converted according to 3.10 and damping coefficients (B_{ij}) according to 3.11:

$$A_{ij} = \rho \cdot L^k \cdot \tilde{A}_{ij} \quad (3.10)$$

$$B_{ij} = \rho \cdot L^k \cdot \tilde{B}_{ij} \cdot \omega \quad (3.11)$$

where

$$\begin{aligned} k &= 3 \text{ for } i, j = 1, 2, 3 \\ k &= 4 \text{ for } i = 1, 2, 3, j = 4, 5, 6 \\ k &= 4 \text{ for } i = 4, 5, 6, j = 1, 2, 3 \\ k &= 5 \text{ for } i, j = 4, 5, 6 \end{aligned} \quad (3.12)$$

L is the model scale length, ρ the water density and ω the frequency [4]. For the calculation of those coefficients a value of 1025 kg/m^3 is used for the water density ρ . The value of the L is equal to 1 m.

3.4.3 Extension of the hydrodynamic coefficients

The coefficients are calculated with the use of WAMIT for a specific range of frequency (from 0.1 rad/s to 2.2 rad/s) and for a specific frequency step of 0.05 rad/s . In order to have the total view of the transfer function of the model those coefficients should be extended from 0 to infinity. In this case all the phenomena can be captured. Something like this will be extremely time consuming so for this reason it is decided to reduce this range from 0 to 10 rad/s . After this value all the elements of the transfer function are almost zero, so it is assumed that there are not extra phenomena after this limit value.

A realistic approach of the extension of the A and B values is described below. For the added mass coefficients (A):

$0.00 \leq \omega < 0.1$: It is assumed a linear interpolation of a line which connect the two first points (values of 0.05 rad/s and 0.01 rad/s)

$0.1 \leq \omega < 2.20$: Values from WAMIT are used

$2.20 \leq \omega < 10.00$: The A values are assumed to be the same with the value of the coefficient for frequency 2.2 rad/s

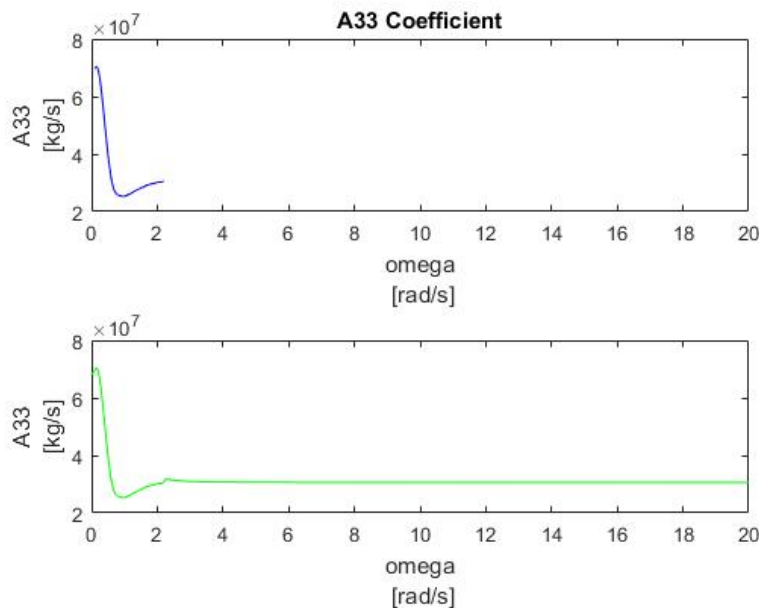


Figure 3.1: A-values from WAMIT and extended A-values.

For the damping coefficients (B):

$0.00 \leq \omega < 0.1$: It is assumed a linear interpolation between zero (for 0 rad/s) and the first $B(\omega)$ value for 0.05 rad/s

$0.1 \leq \omega < 2.20$: Values from WAMIT are used

$2.20 \leq \omega < 10.00$: $B(\omega)$ is assumed to reduce as ω^{-5} in order to reach zero values at high frequencies

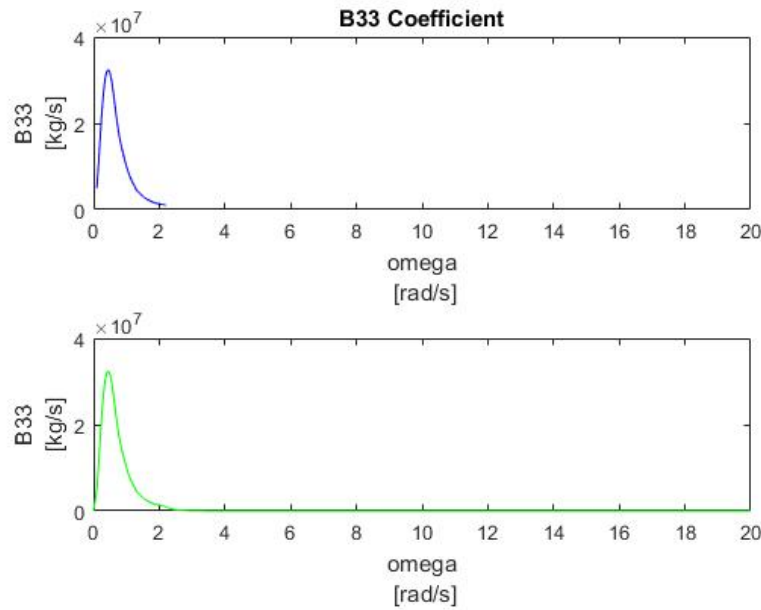


Figure 3.2: B-values from WAMIT and extended B-values.

3.4.4 Hydrostatic coefficients

The hydrostatic coefficients are shown in the following stiffness matrix:

$$K = \begin{bmatrix} 0 & 0 & 0 & 0 & 0 & 0 \\ 0 & 0 & 0 & 0 & 0 & 0 \\ 0 & 0 & K_{33} & K_{34} & K_{35} & 0 \\ 0 & 0 & K_{43} & K_{44} & K_{45} & 0 \\ 0 & 0 & K_{53} & K_{54} & K_{55} & 0 \\ 0 & 0 & 0 & 0 & 0 & 0 \end{bmatrix} \quad (3.13)$$

The non-zero values are calculated again with the help of WAMIT and they are dimensionless. So they should be converted with the following procedure:

$$\begin{aligned} K_{3,3} &= \rho \cdot g \cdot L^2 \cdot \tilde{K}_{3,3} \\ K_{3,4} &= \rho \cdot g \cdot L^3 \cdot \tilde{K}_{3,4} \\ K_{3,5} &= \rho \cdot g \cdot L^3 \cdot \tilde{K}_{3,5} \\ K_{4,4} &= \rho \cdot g \cdot L^4 \cdot \tilde{K}_{4,4} \\ K_{4,5} &= \rho \cdot g \cdot L^4 \cdot \tilde{K}_{4,5} \\ K_{5,5} &= \rho \cdot g \cdot L^4 \cdot \tilde{K}_{5,5} \end{aligned} \quad (3.14)$$

where $K(i,j)=K(j,i)$ for all i,j . For all the other values of the indices i,j , $K(i,j)=0$. For the calculation of those coefficients the same values of water density ρ and model scale length [4].

3.5 Creating the model

3.5.1 State space system

A state-space representation is a mathematical model of a physical system as a set of input, output and state variables related by first-order differential equations. These variables should be expressed in a



vector form. The most general state-space representation of a linear system is written in the following form:

$$\dot{x} = A \cdot x + B \cdot u \quad (3.15)$$

$$y = C \cdot x + D \cdot u \quad (3.16)$$

where the symbols are:

x = state vector

y = output vector

u = input vector

A = state or system matrix

B = input matrix

C = output matrix

D = feed through matrix

The first equation gives the state equation (3.15) and the second is called the output equation (3.16).

3.5.2 Creating a Single Input Single Output Model

The next step is to transfer the equation of the motion in the frequency domain. If the displacement x in the equation 3.2 is substituted by the particular solution of the form [6]:

$$x = X \cdot e^{i\omega t} \quad (3.17)$$

the equation 3.2 will result in the following form:

$$-(M + A(\omega)) \cdot \omega^2 \cdot X + i \cdot B(\omega) \cdot \omega \cdot X + K \cdot X = F \quad (3.18)$$

Solving for the X the result is :

$$X = (-(M + A(\omega)) \cdot \omega^2 + i \cdot B(\omega) \cdot \omega + K)^{-1} \cdot F \quad (3.19)$$

where the

$$(-(M + A(\omega)) \cdot \omega^2 + i \cdot B(\omega) \cdot \omega + K)^{-1} = H \quad (3.20)$$

is called the transfer function. The transfer function is a mathematical representation to describe the motions on the left hand side (X) for any force vector (F). It is a property of the system and it does not change with time but it shows the response of the system for any frequency value.

In Figure 3.3 the transfer function of each one of the 36 elements of the equation of motion can be seen. The transfer functions are plotted for the frequency range from 0 *rad/s* to 10 *rad/s* since after this frequency the values of all the transfer functions are zero. A quick way of ensuring if these transfer functions are correct is the check of the symmetry. Observing the Figure 3.3 it can be seen that the symmetrical elements around the diagonal are identical.

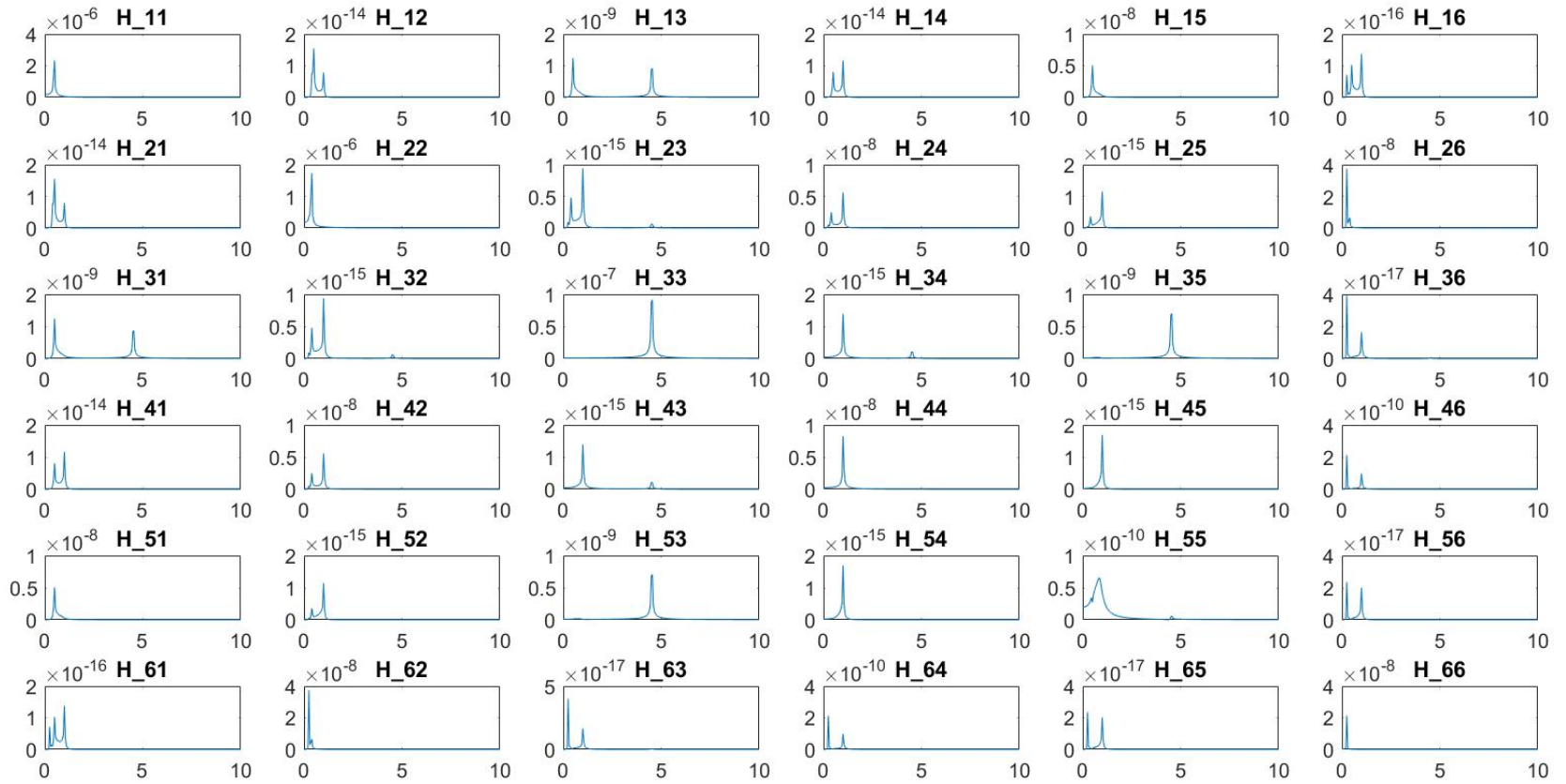


Figure 3.3: Transfer functions of the 36 elements.

The next step is the creation of the approximate system (AS). Initially each element of the transfer function matrix should be converted into a fraction with one polynomial in the numerator and one in the denominator. For this purpose the Matlab command 'invfreqs' is used. In order to have a stable solution of the system the roots of the polynomial in the denominator should have negative real parts. Otherwise the solution becomes unstable. For this reason there is a first check of the sign of the real part of each root of all the elements of the transfer function. If one of the roots has a positive real part then a different polynomial in the denominator should be used. Another necessary check is one regarding the coefficients of both the numerator and the denominator. In some cases it is quite difficult to find two polynomials to describe precisely the transfer function curve. For this reason in some cases Matlab find quite large coefficients to describe this situation. If these values are larger than a value around 100 then there are instabilities in the vessel model. Thus an extra check should be included in the model in order to ensure that the results from the vessel model are correct.

Since the matrix of the transfer function is a 6 by 6 the elements of the transfer function has 36 elements. Thus this procedure should be followed for 36 times. After creating these 36 fractions then the inverse procedure should be followed in order to create functions. This can be achieved with the help of the Matlab command 'freqs'. The following step is the comparison between this approximate system and the original transfer function. This comparison can be easily done by plotting the real and the imaginary part of each element of the approximate system function together with the same element of the original transfer function of the system in a frequency range.

If the comparison has bad results then the order of the polynomials in the numerator and denominator should be increased but always with keeping in mind that the system should be stable, so the roots of the polynomial of the denominator should have negative real part. A comparison between the original and the approximate system for the pitch motion can be seen in Figure 3.4. The yellow and the magenta line describes the real and the imaginary part of the original system respectively. The blue and the red line describes the real and the imaginary part of the approximate system.

As it can be observed in the following Figure there are some small oscillations of the values of the real and the imaginary parts of the original system around 0.5 and 4.5 rad/s. These small peaks are caused by the coupling of the degrees of freedom. In this case, the real and the imaginary parts of roll motion are shown. Roll is coupled with sway and heave. As it can be seen in Figure 3.3, at 0.5 rad/s there is the peak of surge motion (H_11) and at 4.5 rad/s is the peak of the heave motion (H_33).

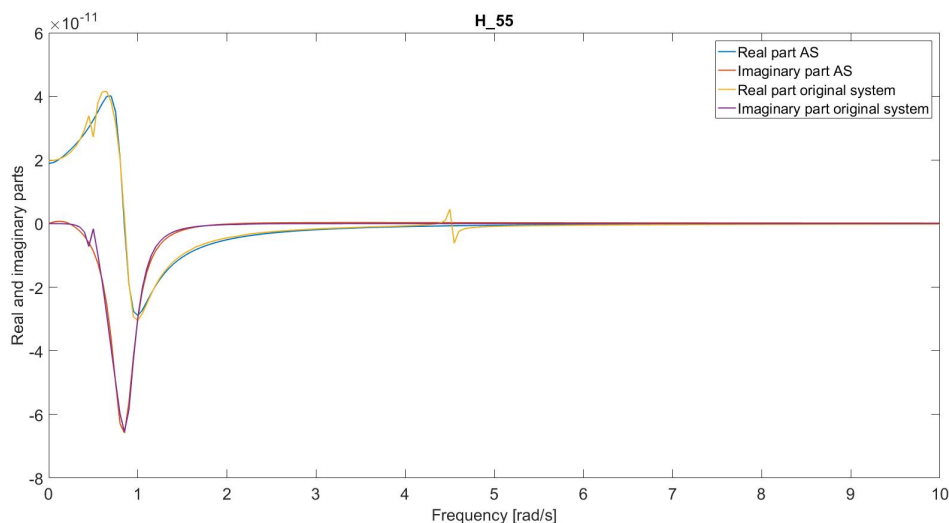


Figure 3.4: Comparison between real and approximate program.

After this, the transfer in time domain and the construction of the state space systems follows. With the use of the Matlab command 'tf2ss' the four matrices of the state space (A,B,C,D) for each element are created based on the coefficients of the polynomial of numerator and denominator. So at the end 36 different state space systems are created, one for each element of the transfer function.

3.5.3 Creating a Multi Input Multi Output Model

The next step is the combination of all these state space systems in order to solve the equation of motion of the vessel. Since the subsystems are independent and have no interconnections, they can be directly combined into a single model simply by defining the new state, input, output and feed through matrices [7]. The control vectors to these systems are defined in terms of the input vectors w_1 and w_2 , using the input selection matrices F_1 and F_2 .

$$u_1 = F_1 \cdot w_1 \quad (3.21)$$

$$u_2 = F_2 \cdot w_2 \quad (3.22)$$

The control, state and observation vectors are defined to include all elements contained in the subsystem models.

$$\begin{aligned} u &= \begin{bmatrix} \dot{x}_1 \\ \dot{x}_2 \end{bmatrix} \\ x &= \begin{bmatrix} \dot{x}_1 \\ \dot{x}_2 \end{bmatrix} \\ y &= \begin{bmatrix} \dot{x}_1 \\ \dot{x}_2 \end{bmatrix} \end{aligned} \quad (3.23)$$

If the system state equations are expressed in terms of the input vectors and the input selection matrices, the equations for the system become

$$\begin{aligned} \left. \begin{aligned} \dot{x}_1 &= A_1 \cdot x_1 + B_1 \cdot u_1 \\ y_1 &= C_1 \cdot x_1 + D_1 \cdot u_1 \end{aligned} \right\} = System1 \\ \left. \begin{aligned} \dot{x}_2 &= A_2 \cdot x_2 + B_2 \cdot u_2 \\ y_2 &= C_2 \cdot x_2 + D_2 \cdot u_2 \end{aligned} \right\} = System2 \end{aligned} \quad (3.24)$$

$$w_1 \rightarrow F_1 \rightarrow \left\{ \begin{aligned} \dot{x}_1 &= A_1 \cdot x_1 + B_2 \cdot u_1 \\ y_1 &= C_1 \cdot x_1 + D_1 \cdot u_1 \end{aligned} \right\} \rightarrow y_1 \quad (3.25)$$

$$w_2 \rightarrow F_2 \rightarrow \left\{ \begin{aligned} \dot{x}_2 &= A_2 \cdot x_2 + B_2 \cdot u_2 \\ y_2 &= C_2 \cdot x_2 + D_2 \cdot u_2 \end{aligned} \right\} \rightarrow y_2 \quad (3.26)$$

Taking into account the logic flow of equations 3.25 and 3.26 and using the previous definitions, the new state equation is represented by the following equations.

$$\begin{bmatrix} \dot{x}_1 \\ \dot{x}_2 \end{bmatrix} = \begin{bmatrix} A_1 & 0 \\ 0 & A_2 \end{bmatrix} \begin{bmatrix} x_1 \\ x_2 \end{bmatrix} + \begin{bmatrix} B_1 F_1 & 0 \\ 0 & B_2 F_2 \end{bmatrix} \begin{bmatrix} w_1 \\ w_2 \end{bmatrix} \quad (3.27)$$

$$\begin{bmatrix} y_1 \\ y_2 \end{bmatrix} = \begin{bmatrix} C_1 & 0 \\ 0 & C_2 \end{bmatrix} \begin{bmatrix} x_1 \\ x_2 \end{bmatrix} + \begin{bmatrix} D_1 F_1 & 0 \\ 0 & D_2 F_2 \end{bmatrix} \begin{bmatrix} w_1 \\ w_2 \end{bmatrix} \quad (3.28)$$

This procedure is followed for the 36 elements of the transfer function in this case. The zero sub matrices are of an order appropriate for the specific application.

After creating the 4 matrices (A,B,C,D) there is one system with a different number of degrees of freedom (not 6 as the vessel has). The new number of the degrees of freedom will be the summation of the

order of the polynomials which are used for the fitting of each element of the transfer function. These degrees of freedom do not have a specific physical meaning but they just help in the construction of the approximation system. In the continue those 36 state space systems are inserting in the Matlab ode solver as one big state space with only 4 matrices. The input for each state space is the force for the corresponding element of the transfer function. Following the linear superposition the outputs of the system for the vessel's motion is calculated as the summation of the outputs of the state space systems for each transfer function element. For example for the calculation of each degree of freedom i (where $i=1:6$, for the 6 degrees of freedom of the vessel) the following procedure is used:

$$u_i = H_{i1} \cdot F_1 + H_{i2} \cdot F_2 + H_{i3} \cdot F_3 + H_{i4} \cdot F_4 + H_{i5} \cdot F_5 + H_{i6} \cdot F_6 \quad (3.29)$$

Where the H matrix is the transfer function matrix and F the force vector. So every time when a displacement of one degree of freedom is used (both inside and outside the ode function), it is calculated like this.

3.6 Model validation

3.6.1 Check the model's stability

In order to ensure that the model works properly some validations checks should be made. There were some problems with instabilities during the construction of the approximation system, so it is quite necessary and useful to check the model.

The first check for the stability of the model is the output of the model. If the values are logical and they do not go to infinity is a first indication that the model is at least stable. The next step in order to validate the stability of the model is the check of the stability of the vessel's motions with applying some random initial conditions and without any external forces (only the restoring forces). After some time the motions of the vessel should be reduced and finally the vessel should reach a static equilibrium. For this specific model the center of gravity is placed at a location with zero co-ordinates and angles, so all the displacements and the rotations should become zero after some time. The value should become zero despite the initial conditions. In this case the following initial conditions are selected as an example:

$$q_0 = [0.16, 0.57, 0.21, 0.1, -0.05, 0] \quad (3.30)$$

The units for the three first initial conditions (surge,sway,heave) are meters and the units for the rest (roll,pitch, yaw) are radians.

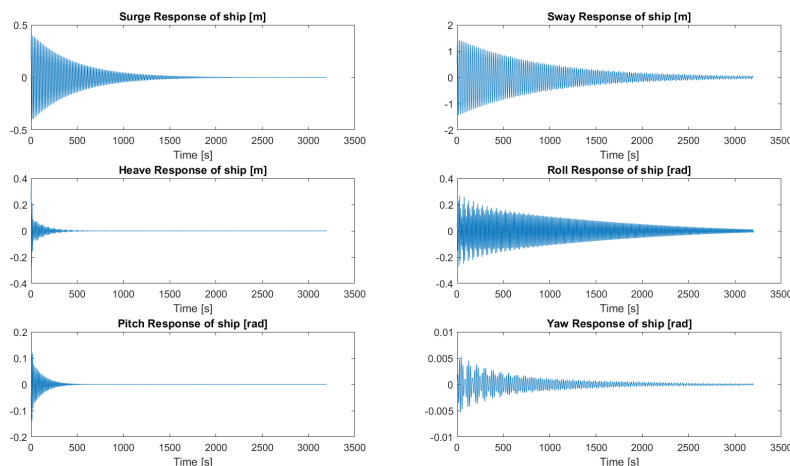


Figure 3.5: Motions of the vessel after applying initial conditions.

As it can be shown from the Figure above the motions of the vessel decrease with the time. All the motions reach zero value after some time. So it can be proved that there are no instabilities in the system. This can be considered as a second check after the check of the real part of the roots of the denominator as it referred in 3.5.2.

3.6.2 Comparison between 2 Matlab models

The next step in order to check if the model is correct is the validation of the results using the results of a different model. If the results are quite close, the approximate system developed in this project is correct, since the other one is a proved program. In this case a Matlab model (provided by my supervisor Ir. C. Keijdener) is adopted with which the convolution scheme is used for the solution of the same problem. The convolution scheme is the solution of the time consuming convolution integral which is referred in the section 3.1.2.

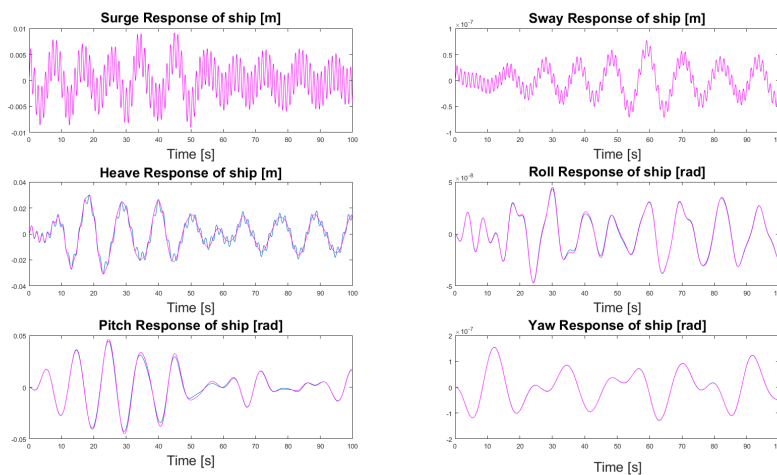


Figure 3.6: Comparison of the results of the two models.

As it can be seen from the Figure 3.6 the two outputs are quite close. The original model (blue line) is an approximate model so it is logical to have some differences but it is a good approximation of the reality and it can be used for the solution of this problem. Despite the fact that the convolution model (magenta line) is more accurate it is quite slower than the original model. At this moment only the vessel with some restoring stiffness in each direction is modeled. Because of the fact that more elements (like the spudpoles and the hydraulic cylinders) will be inserted into the model, it is decided to choose the original model (approximate model) since it is faster and quite accurate.



4 Compensation system

4.1 Hydraulic cylinders

A hydraulic cylinder is a mechanical actuator that is used to give an unidirectional force through a unidirectional stroke. They get their power from pressurized hydraulic fluid, which is typically oil. The hydraulic cylinder consists of a cylinder barrel, in which a piston connected to a piston rod moves back and forth. In this case a double acting cylinder will be used. This type of cylinder is also known as a differential cylinder. Differential cylinders are constructed with two opposed piston surfaces, meaning that they can work in two directions. Because of the presence of the piston rod, this type of cylinder has two different working surfaces, which generally lead to differential piston speeds.

When the piston moves towards the right side (Figure 4.1) then fluid goes out from the right valve and at the same time fluid will be inserted in the cylinder to the left valve. Exactly the opposite procedure will be followed if the piston moves towards the left side of the cylinder.

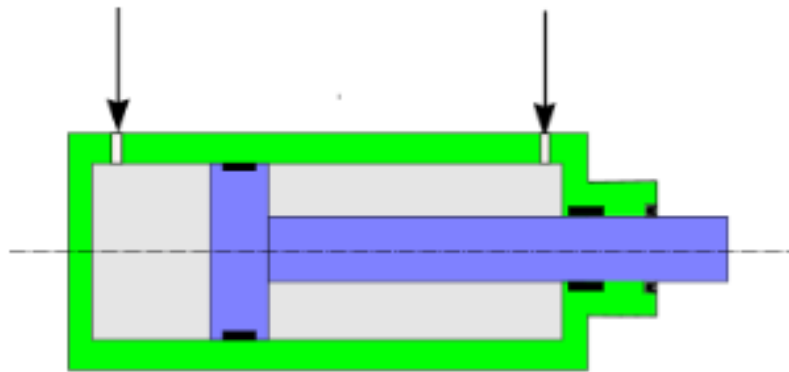


Figure 4.1: Double acting hydraulic cylinder.

In this type of cylinders both bottom and rod end are driven, so it can work in both directions. The hydraulic cylinder can be modeled like a spring with a specific hydraulic stiffness [8]. This spring reacts in the opposite direction causing a reduction in the movement of the vessel. In this specific project the hydraulic cylinders will be attached both in the vessel and in the spudpoles, so the relative motion of these two parts should be taken into account for the calculation of the forces.

4.2 Hydraulic stiffness of the system

As it is described in the previous section the hydraulic cylinder will work as a spring with a specific stiffness. The calculation of the hydraulic stiffness is based on several factors. Analytically the hydraulic stiffness (C_o) for a double acting hydraulic cylinder is calculated as follows[8]:

$$C_o = \frac{E \cdot (\sqrt{A_1} + \sqrt{A_2})^2}{S + \frac{V_{p1}}{A_1} + \frac{V_{p2}}{A_2}} \quad (4.1)$$

Where the symbols are:

C_o = hydraulic stiffness

E = fluid elasticity

A = Area of cylinder

S = Stroke length

V_p = Volume of the pipe

There are two different areas (A) in the hydraulic cylinder. The first one is on the left of the cylinder and it is equal to the whole area of the piston. The second one is on the right side of Figure 4.1 which is the area of the piston minus the area of the rod. For this reason there are two different areas in the calculation of the hydraulic stiffness. Specifically for this project a cylinder with a diameter of 0.5 m and a stroke of 8 m is selected. The two pipes have a diameter of 0.06 m and a length of 10 m . The hydraulic stiffness of each cylinder is calculated based on the formula 4.1 equal to $1.26 \cdot 10^5\text{ kN/m}$.

4.3 Configuration of the system

As it was discussed in the previous chapters the compensation of the vessel's motion will be achieved through two identical compensation systems which will be attached both on the vessel and the spudpoles. The aim of each system is to compensate the motion of the vessel in each degree of freedom. Each system consists of hydraulic cylinders in the three directions (x,y,z) which will create forces in order to reduce the motion of the vessel.

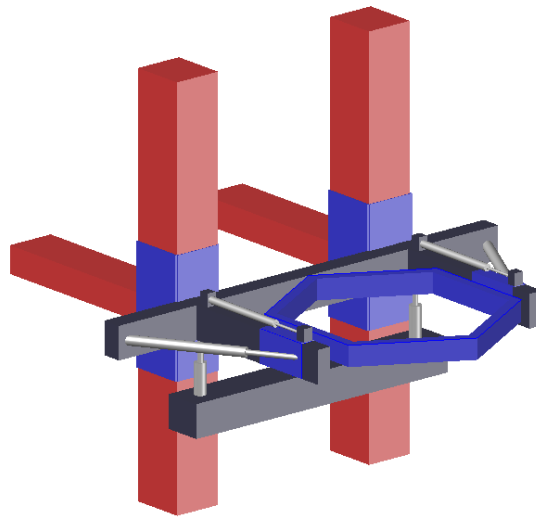


Figure 4.2: Compensation System.

As it can be observed in Figure 4.2 each system consists of two cylinders in x -direction, two in the y -direction and two in the z -direction. Each of the cylinder will reduce the displacements of the vessel in the direction of the orientation of the cylinder. Moreover the cylinders in the z -direction will reduce the pitch and roll rotations of the vessel and on the other hand the cylinders in x and y -direction will reduce the yaw motion of the vessel. The red part of the system will be placed on the deck of the vessel and the piles will be placed inside the blue frame in a vertical position. It will be exactly the same system in both sides of the vessel.

4.4 Location of the compensation system

As far as now the motion compensation of the vessel is based in flippers which are placed in the two sides of the vessel preventing mainly the roll motion of the vessel. These flippers are connected with the vessel at the one third of the vessel's length and they can be attached to the vessel in several z positions. For this reason the hull at this point is strengthened. The two compensation systems will be placed at the same points in order to avoid any damage at the hull of the vessel during the operation.

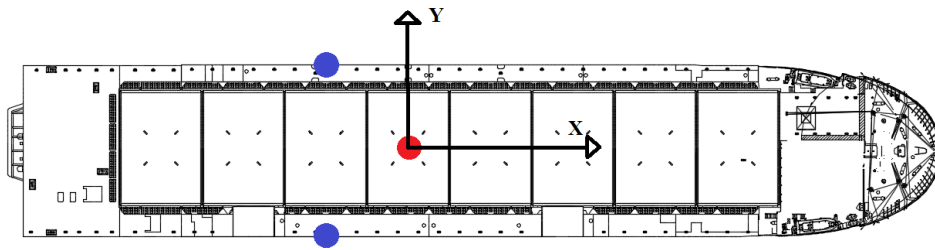


Figure 4.3: Location of the compensation systems.

The definition of the two axis, x and y, can be seen in Figure 4.3. The z axis is vertical on this plane. The two compensation systems are indicated with the blue dots. The upper one will be called the left compensation system and the one in the lower part of the Figure will be called the right one. Specifically the exact location of the poles are:

	Left compensation system	Right compensation system
X - coordinate (m)	-15	-15
Y - coordinate (m)	13.5	-13.5
Z - coordinate (m)	5	5

Table 4.1: Area definition.

A better representation of the whole compensation system can be seen in the following Figure.

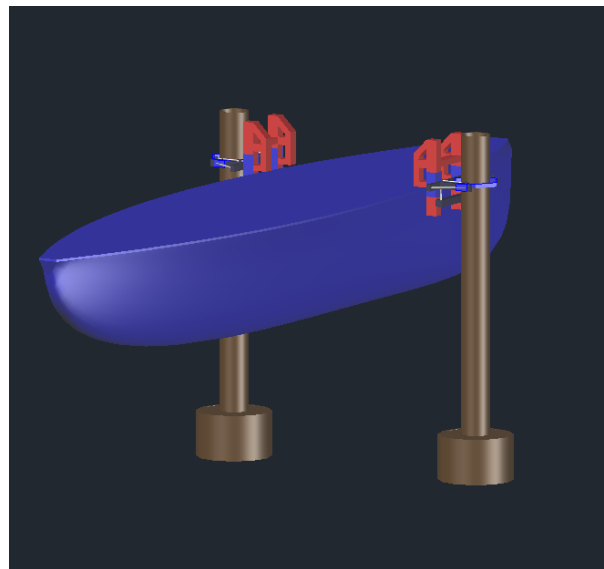


Figure 4.4: The compensation systems.

4.5 Installation process

In the following section the whole process of the installation of the spudpoles for the stabilization of the vessel will be described. A visualization of this process is shown in the Figures 4.5-4.8. Firstly the two poles are in horizontal position and they are laying on the deck. They are not already in the vertical position because in this case there will be an extra drag force from the sea resulting in the reduction of the vessel speed.



Figure 4.5: The sailing phase.

When the vessel reaches the place for the installation of the transition pieces the second phase begins. This phase is called upending. The upending procedure will be done by the help of hydraulic cylinders. These cylinders will be placed on the deck of the vessel and they will be connected at the upper end of the compensation frame (the upper point of the red frame in Figure 4.2). With the help of these cylinders the whole frame can rotate and move the poles from the horizontal position to a vertical one. The poles start to turn and take the vertical position.



Figure 4.6: The upending phase.

The following phase is the lowering phase. The poles with the help of a jacking system or guided by the cranes of the vessels will start to lower and reach the seabed.

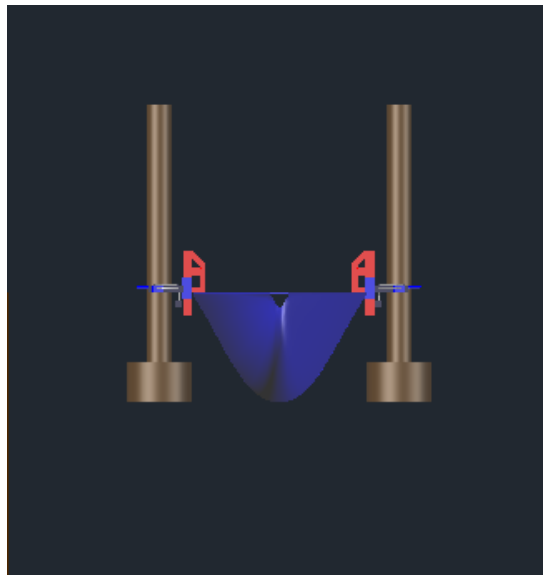


Figure 4.7: The lowering phase.

The final phase is the penetration of the poles into the seabed. As it is described in Chapter 2 the poles will be inserted in the soil with the help of suction. With the use of pumps, under-pressure will be enabled inside the bucket and in combination with the self-weight the bucket will start to insert the soil. This procedure will continue until the whole bucket will be inside the soil. From this moment the vessel is quite stable and the installation process can start.

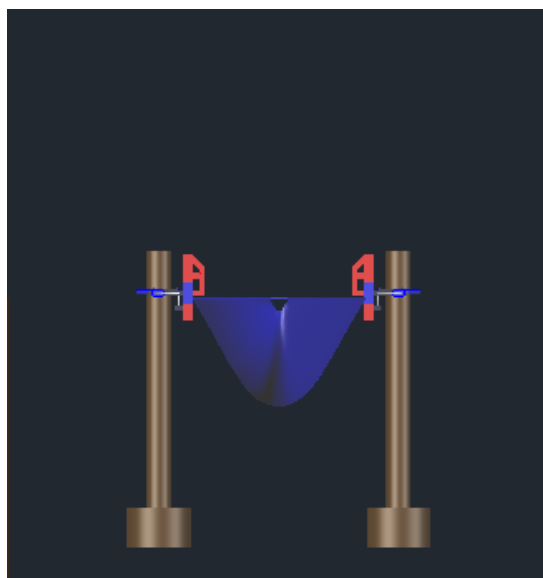


Figure 4.8: The penetration phase.

When the installation process is over, the inverse procedure will occur. The spudpoles will be extracted from the soil with the help of the pumps again. Afterwards, the spudpoles will be lifted and with the help of the cylinders in the deck the whole frame will rotate in order to bring the spudpoles in the horizontal position. The vessel will sail for the next location and then the same procedure will be followed.



5 Wave Loads

5.1 Wave Loading on the vessel

5.1.1 Regular waves

For the analysis of a wave field the regular (harmonic) waves will be analyzed first. The elevation of the water surface at a specific location (x,y) due to a harmonic wave is described from the following equation :

$$\zeta = \zeta_a \cdot (\omega \cdot t - k \cdot x \cdot \cos(\mu) - k \cdot y \cdot \sin(\mu)) \quad (5.1)$$

Where the symbols are:

ζ = surface elevation

ζ_a = wave amplitude

ω = wave frequency

t = time

k = wave number

μ = wave heading

So the wave elevation at the center of gravity (x=0,y=0) will be described from the following equation:

$$\zeta = \zeta_a \cdot \cos(\omega \cdot t) \quad (5.2)$$

5.1.2 Irregular waves

In the real life a wave field is not a harmonic wave but on the contrary it is a result of irregular waves. But even in this case this field can be described as a summation of a finite number of propagating regular wave components. Each component has a different amplitude, wave frequency, wave length, phase and direction [9]. The summation of the individual harmonic components results in an irregular wave field. This method is called the superposition principle and it is described by the following equation.

$$\zeta(t) = \sum_{n=1}^N \zeta_{a_n} \cdot \cos(\omega_n \cdot t + \epsilon_n) \quad (5.3)$$

for n= 1...N

where:

ϵ_n = phase of wave component n

The visualization of the superposition principle is shown in the following Figure.

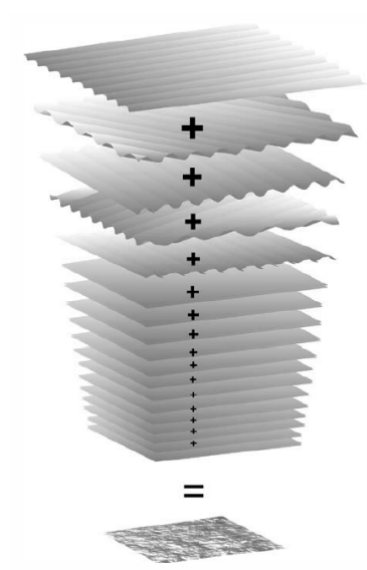


Figure 5.1: The superposition principle.

5.1.3 Dispersion relationship

The relationship between ω and k named dispersion relation for an arbitrary water depth d is described by the following equation

$$\omega^2 = g \cdot k \cdot \tanh(k \cdot d) \quad (5.4)$$

This equation can be used for the calculation of the wave number k , according to the depth and the wave frequency. In the deep waters the equation is quite simple but in this case the water depth will be relatively small (around 30 m) and the equation 5.4 will be used.

5.1.4 Response amplitude operator (RAO)

The force response amplitude operator (RAO) is a transfer function which give the forces and moments of a specific wave for the six degrees of freedom of the vessel. They depend on the frequency and the heading of the wave motion. The values of the RAO are provided by WAMIT for 13 directions (from 0° to 180°) since the vessel is symmetric. The values of WAMIT are dimensionless and they should be converted in SI units according to the follow equation:

$$X_i = \rho \cdot g \cdot \zeta_a \cdot L^m \cdot \tilde{X}_i \quad (5.5)$$

where $m=2$ for $i=1,2,3$ and $m=3$ for $i=4,5,6$.

In Figure 5.2 the RAO for the roll motion as a function of frequency and heading is shown. As it can be observed from this Figure the maximum value of the force is located at 90 degrees heading which is what it is expected.

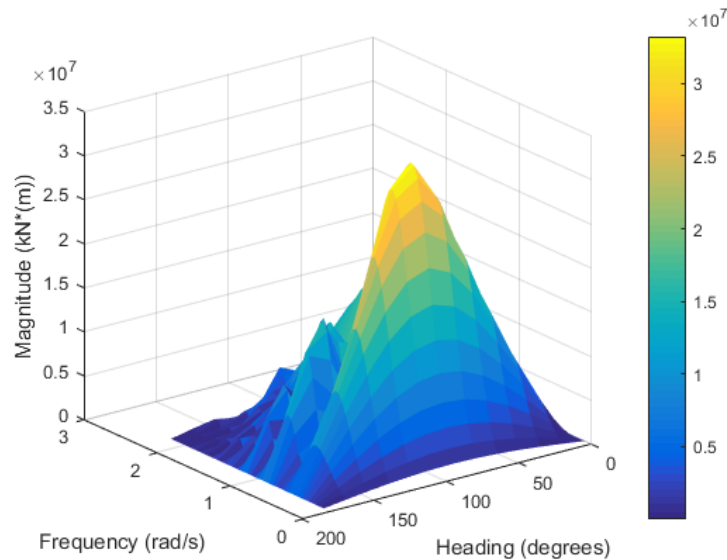


Figure 5.2: RAO for roll motion.

5.1.5 Wave spectrum

A wave spectrum represent a sea state in frequency domain. There are different types of spectra. The main types are the Pierson-Moskowitz (PM) which describes a fully developed sea and the JONSWAP (Joint Open North Sea Project) which represents seas with limited fetch. The North Sea is one of those seas, so the JONSWAP spectrum will be used in this project.

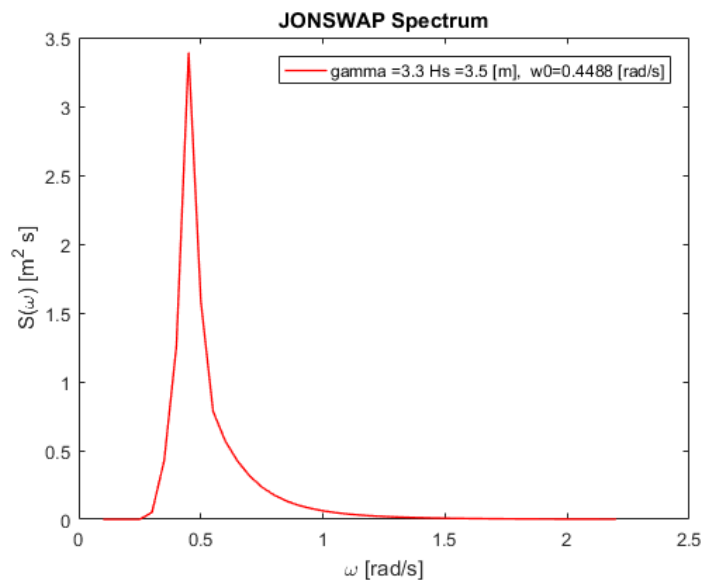


Figure 5.3: JONSWAP spectrum.

In Figure 5.3 a JONSWAP spectrum can be seen, where in the vertical axis the spectral density ($S(\omega)$) and in the horizontal axis the wave frequency are shown. The area under the red line represents the total amount of energy of the wave for the frequency range from 0 to infinity. As it can be observed in the above Figure the values are around 0 for frequencies higher than 2 rad/s . In order to estimate the value of the area under the red line the coming procedure is followed. As it is discussed an irregular wave can be described as a summation of n harmonic waves. The next step is the slicing of the spectrum in n parts.

For each part the value of the spectral density is calculated at the center of each slice. If the number is too high the representation of the spectral density is almost perfect but on the other hand it is a quite time consuming procedure because in each time step infinitely many parts should be added in order to calculate the spectral density.

The discretization will definitely lead to an error in the calculation of the spectral density. To ensure that this error will not be quite big and that will not influence the result in a significant level, it is calculated as a function of the number of frequency components.

$$e = \frac{|\text{Area}_c - \text{Area}_d|}{\text{Area}_c} * 100 \quad (5.6)$$

Where:

Area_c = Area under the spectrum for the continues function

Area_d = Area under the spectrum after the discretization

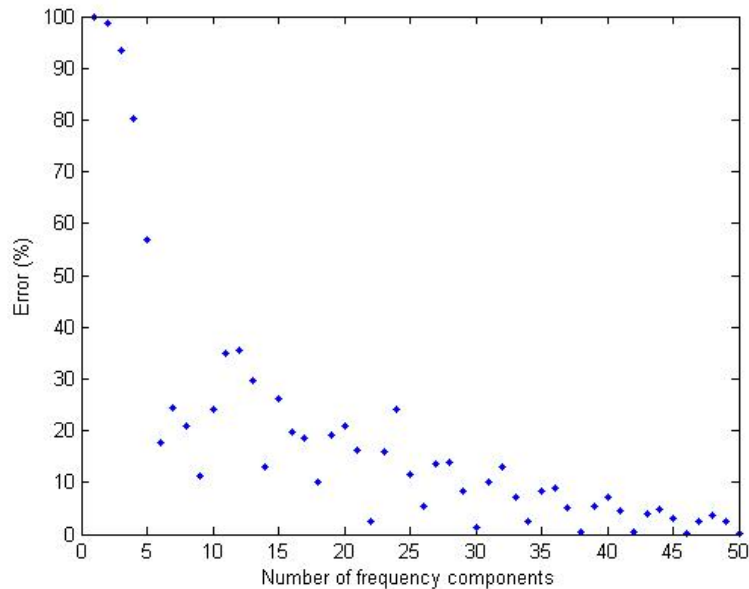


Figure 5.4: Error as a function of frequency components.

As it can be seen from Figure 5.4 the error is significant large for a small number of elements. But if the number of elements increases the error is getting smaller. In order to get a good approximation of the spectral energy and a fully irregular sea state, 40 or more frequency components is a quite good choice. Firstly, 43 frequency components are selected for the representation of the wave spectrum. It is a good approximation of the real spectrum and also it is not so time consuming thus making the model faster.

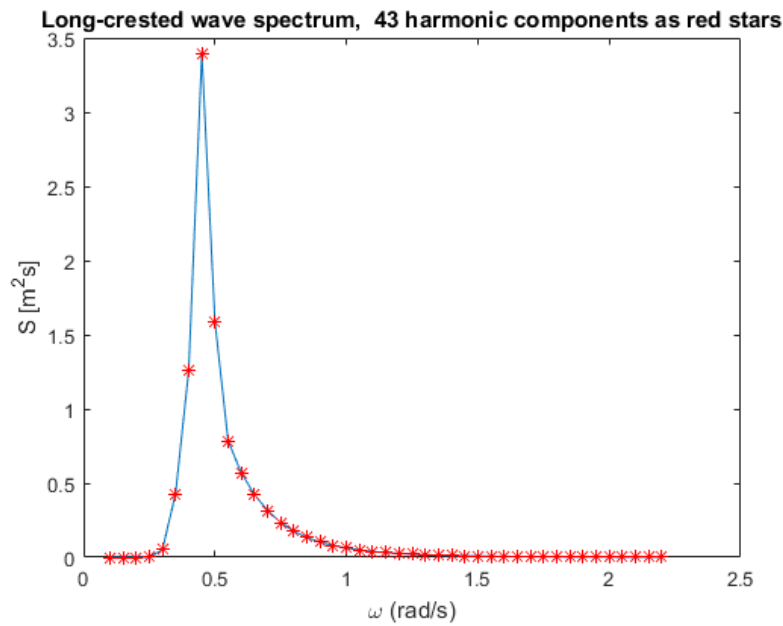


Figure 5.5: Discretized wave spectrum with 43 components.

After the first simulation it was noticed that there was a quite regular pattern and there was not a good representation of the irregular sea state. For this reason it was decided to change the harmonic components to 170. The results were better despite the fact that there was need for extra computational time. The new discretized spectrum can be seen in the next Figure.

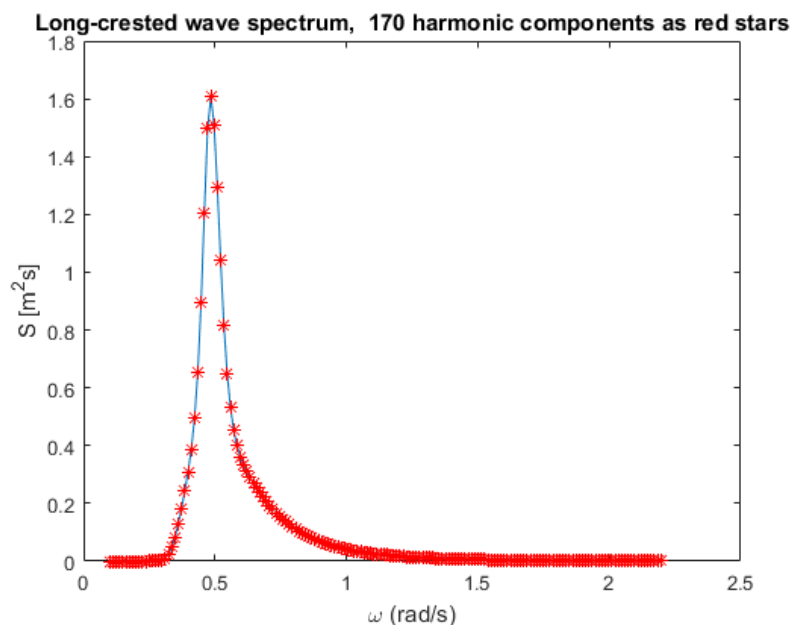


Figure 5.6: Discretized wave spectrum with 170 components.

5.1.6 Diffraction force

For the calculation of the wave forces and moments for each degree of freedom, as it is referred in equation 5.5 the RAO values and the surface elevation are needed. The surface elevation can be calculated for the following equation:

$$\zeta(t) = \sum_{n=1}^N \zeta_{a_n} \cdot \cos(\omega_n \cdot t + \epsilon_n) \quad (5.7)$$

where ϵ_n is a random phase generated for each wave component.

Finally the calculation of the wave forces and moments is made by the equation 5.8

$$F_j = \sum_{n=1}^N RAO_{j,n} \cdot \zeta_{a_n} \cdot \cos(\omega_n \cdot t + \epsilon_n + \phi_{j,n}) \quad (5.8)$$

The extra phase ϕ which is added here depends on the direction of the waves and the values for each direction and frequency are provided from WAMIT.

5.2 Wave Loading on the spudpoles

5.2.1 Wave potential and water particle velocity

The wave potential, depending on the water depth d is given by the following relation :

$$\Phi_w = \frac{\zeta_a \cdot g}{\omega} \cdot \frac{\cosh k(d+z)}{\cosh kd} \cdot \sin(k \cdot x - \omega \cdot t) \quad (5.9)$$

In order to reach the above equation the following assumptions should be made [5]:

- The fluid is inviscid (no viscosity)
- The fluid is homogeneous and incompressible
- The flow is irrotational

The resulting velocity of the wave particles components in the general form can be expressed as:

$$u = \frac{\partial \Phi_w}{\partial x} = \zeta_a \cdot \frac{kg}{\omega} \cdot \frac{\cosh k(d+z)}{\cosh kd} \cdot \cos(k \cdot x - \omega \cdot t) \quad (5.10)$$

$$w = \frac{\partial \Phi_w}{\partial z} = \zeta_a \cdot \frac{kg}{\omega} \cdot \frac{\sinh k(d+z)}{\cosh kd} \cdot \sin(k \cdot x - \omega \cdot t) \quad (5.11)$$

and with a substitution of:

$$kg = \frac{\omega^2}{\tanh kd} \quad (5.12)$$

Derived from the dispersion relation the following formulas for the velocities are reached:

$$u = \zeta_a \cdot \omega \cdot \frac{\cosh k(d+z)}{\sinh kd} \cdot \cos(k \cdot x - \omega \cdot t) \quad (5.13)$$

$$w = \zeta_a \cdot \omega \cdot \frac{\sinh k(d+z)}{\sinh kd} \cdot \sin(k \cdot x - \omega \cdot t) \quad (5.14)$$

where the u is the velocity in x -axis and w the velocity in z -axis.

Also the acceleration of the wave particles in the x -direction and z -direction is given by:

$$a_x = \frac{\partial u}{\partial t} = \zeta_a \cdot \omega^2 \cdot \frac{\cosh k(d+z)}{\sinh kd} \cdot \sin(k \cdot x - \omega \cdot t) \quad (5.15)$$

$$a_z = \frac{\partial w}{\partial t} = -\zeta_a \cdot \omega^2 \cdot \frac{\cosh k(d+z)}{\sinh kd} \cdot \cos(k \cdot x - \omega \cdot t) \quad (5.16)$$

5.2.2 Wave and current velocity

In the region of the North Sea there are currents which influence the motion of the vessel and the wave loads on the spudpoles. It is assumed a current with a steady velocity of 0.5 m/s on the water surface. The vertical profile of the velocity can be calculated by the following distribution:

$$U_c(z) = U_{c0} \cdot \left(\frac{z+d}{d}\right)^a \quad (5.17)$$

Where:

$U_c(z)$ = the current speed at elevation $-d \leq z \leq 0$

U_{c0} = current speed at the water surface

d = sea depth

a = an exponent, equal to 1/7

z = the vertical coordinate, measured positively upwards from the still water level

Based on this formula and on equation 5.13 the velocity of the water particles due to both waves and currents can be calculated. For a depth of 30m and a wave with height 2.5m and a period of 13 seconds the velocity and the acceleration can be seen in the below Figures. The water particles horizontal velocity profiles are presented in the following Figure:

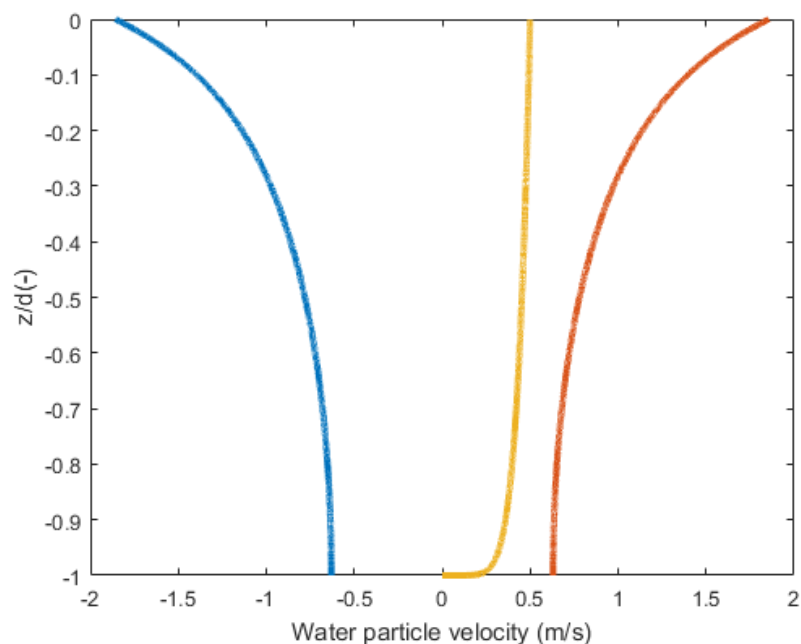


Figure 5.7: Water velocity profile as a function of z/d

In the Figure 5.7 there are separate drawings for the velocities due to wave and current. The red line represents the current velocity. The blue and the yellow line represents the maximum and minimum wave velocities respectively. In the next Figure the total maximum and minimum velocities are presented. The blue line shows the maximum total velocity and the red line the minimum total velocity.

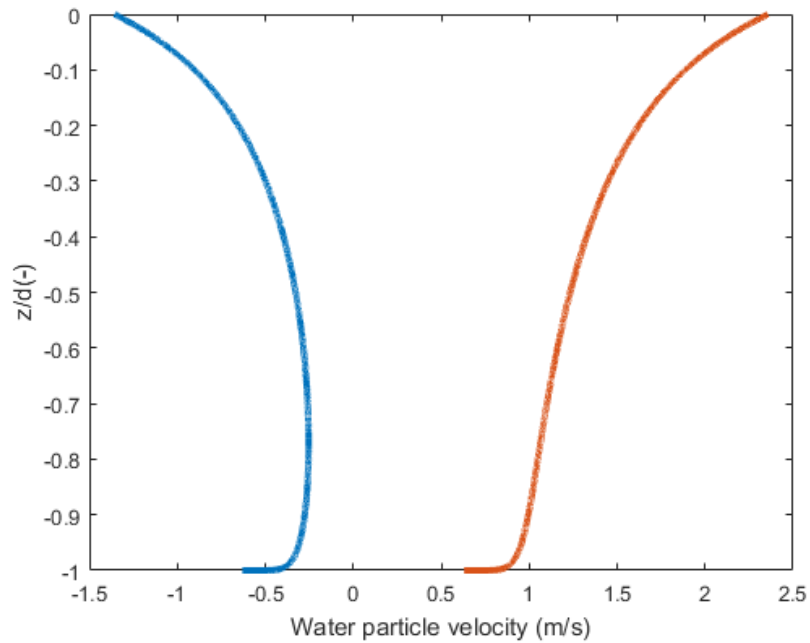


Figure 5.8: Total water velocity profile as a function of z/d

The next Figure shows the profile of the water particles acceleration. It is worth mentioning that the current has no contribution to the acceleration since a steady velocity it is assumed.

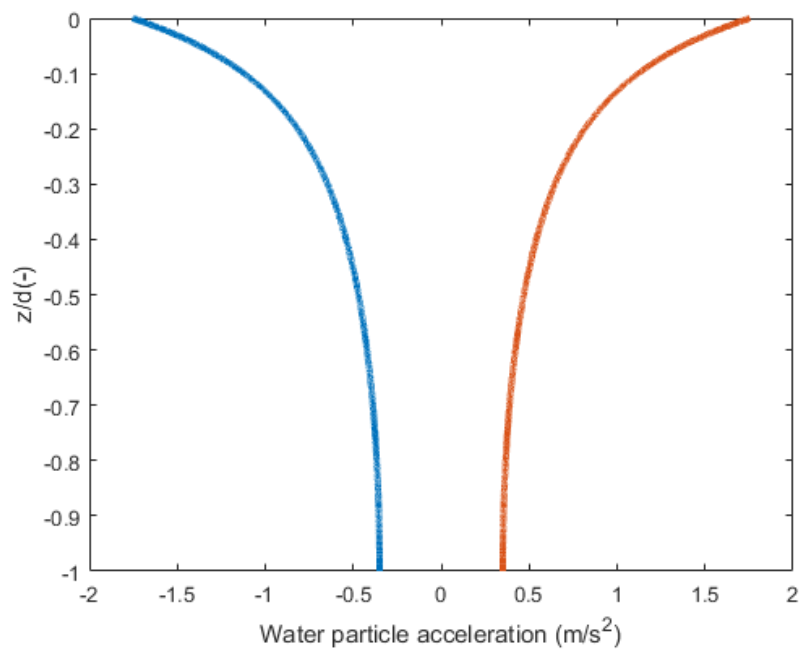


Figure 5.9: Water acceleration profile as a function of z/d

In the above Figure the maximum acceleration is represented by the blue line and the minimum by the red.

5.2.3 Morison equation

The Morison equation is an equation for the inline force on a body in oscillatory flow. It is the sum of two separate and well known phenomena, the drag in a current and the hydrodynamic inertia in an accelerating flow. In an oscillatory flow with flow velocity $u(t)$, the Morison equation gives the inline force parallel to the flow direction according to the following equation [5]:

$$F(t) = \rho \cdot C_M \cdot V \cdot \dot{u}(t) + \frac{1}{2} \cdot \rho \cdot C_D \cdot A \cdot |u(t)| \cdot u(t) \quad (5.18)$$

Where:

$\mathbf{F}(t)$ = Total force on the body

$\dot{u}(t)$ = Acceleration flow

$\mathbf{F}_I = \rho \cdot C_M \cdot V \cdot \dot{u}(t)$ = Inertia Force per meter

$\mathbf{F}_D = \frac{1}{2} \cdot \rho \cdot C_D \cdot A \cdot |u(t)| \cdot u(t)$ = Drag Force per meter

C_A = Added mass coefficient

$C_M = 1 + C_A$ = Inertia coefficient

C_D = Drag coefficient

\mathbf{A} = Cross-sectional area of the body perpendicular to the flow direction

\mathbf{V} = Volume of the body

The equation 5.18 is referred to a motionless body. If the body moves then this motion should be taken into account in the calculation of the forces on it. The new formula for the calculation of the forces in the moving body is:

$$F(t) = \rho \cdot V \cdot \dot{u}(t) + \rho \cdot C_A \cdot V \cdot (\dot{u}(t) - \ddot{x}(t)) + \frac{1}{2} \cdot \rho \cdot C_D \cdot A \cdot |u(t) - \dot{x}(t)| \cdot (u(t) - \dot{x}(t)) \quad (5.19)$$

Where:

\mathbf{x} = the displacement of the moving body

$\dot{\mathbf{x}}$ = the velocity of the moving body

$\ddot{\mathbf{x}}$ = the acceleration of the moving body

Another key point is that the Morison force is a distributed force over the length of the body in the flow. So it is a force calculated for unit length and for this reason it should be multiplied at the end by the total length of the structure (in this case, the spudpoles). Because of the discretization of the spudpoles, the force for each element should be multiplied by the length of the element.

5.2.4 Implementation of the acceleration term in the Morison equation

In the equation 5.19 there is a term which contains the acceleration of the moving body. In order to implement this in the Matlab model it is decided to place the term $\rho \cdot C_A \cdot V \cdot \ddot{x}(t)$ in the mass matrix of the spudpoles (as an added mass term) outside the ode function.



6 Modelling of the spudpoles

6.1 Implementation of the spudpoles

The two spudpoles are a quite important part of the general system. They will be connected via hydraulic cylinders to the vessel in order to receive the loads from the motion of the vessel and transfer them through their own body into the soil with the final goal to reduce the motion of the vessel in the 6 degrees of freedom. Each spudpole can be considered as a vertical Euler-Bernoulli beam with two ends. The first end is assumed clamped at the sea bottom and the second one (tip of the beam) is free. At this point at the tip of the beam the hydraulic cylinders will be attached and they will connect the beam with the vessel. In order to calculate the deflections and rotations of the spudpole it could be considered as a cantilever beam. For better accuracy and in order to solve the problem numerically using ode Matlab function, the beam needs to be discretized [10]. The central finite difference scheme is used to approximate the derivatives with respect to space and after applying the boundary conditions for the two ends, the resulting equation of motion of the beam is (for a discretization of 7 number of nodes for instance):

$$\rho \cdot A \cdot \begin{bmatrix} 1 & 0 & 0 & 0 & 0 & 0 \\ 0 & 1 & 0 & 0 & 0 & 0 \\ 0 & 0 & 1 & 0 & 0 & 0 \\ 0 & 0 & 0 & 1 & 0 & 0 \\ 0 & 0 & 0 & 0 & 1 & 0 \\ 0 & 0 & 0 & 0 & 0 & 1 \end{bmatrix} \cdot \begin{bmatrix} \ddot{w}_2 \\ \ddot{w}_3 \\ \ddot{w}_4 \\ \ddot{w}_5 \\ \ddot{w}_6 \\ \ddot{w}_7 \end{bmatrix} + \frac{EI}{l^4} \cdot \begin{bmatrix} 7 & -4 & 1 & 0 & 0 & 0 \\ -4 & 6 & -4 & 1 & 0 & 0 \\ 1 & -4 & 6 & -4 & 1 & 0 \\ 0 & 1 & -4 & 6 & -4 & 1 \\ 0 & 0 & 1 & -4 & 5 & -2 \\ 0 & 0 & 0 & 2 & -4 & 2 \end{bmatrix} \cdot \begin{bmatrix} w_2 \\ w_3 \\ w_4 \\ w_5 \\ w_6 \\ w_7 \end{bmatrix} = \begin{bmatrix} F_2 \\ F_3 \\ F_4 \\ F_5 \\ F_6 \\ F_7 \end{bmatrix} \quad (6.1)$$

Where the symbols are:

ρ = density of the material of the beam

A = the cross section area of the beam

E = the elastic modulus of the beam

I = the area moment of inertia of the beam cross-section

l = the length of each element

w = the deflection of each node

F = the force applied on each node

For better understanding the 1st point of the discrete beam is the fixed one in the bottom of the structure, so it has no displacement or velocity. The analytical procedure in order to reach the equation 6.1 with the application of the specific boundary conditions can be found in the Appendix B. As regards the force vector, the force on the tip of the beam will be the force from the hydraulic cylinder and the forces on the nodes underwater will be the wave forces (from the Morison equation).

For the validation of the finite difference scheme a comparison was performed with the result of the analytical solution for the deflection of a cantilever beam. Firstly, the static equilibrium of the cantilever beam can be obtained as follows:

$$x_{static} = [K]^{-1} \cdot F \quad (6.2)$$

Where:

K = stiffness matrix

F = force vector

The deflection of a cantilever beam for a concentrated force, applied at the free end, can be calculated based on the following equation:

$$y = \frac{F \cdot x^2}{6EI} \cdot (3 \cdot l - x) \quad (6.3)$$

Where:

y = deflection of the beam

x = position along the length of the beam

l = length of the beam

For the same applied force at the top of the cantilever beam, the deflection curves based on finite differences scheme and the analytical solution can be seen in the following Figure.

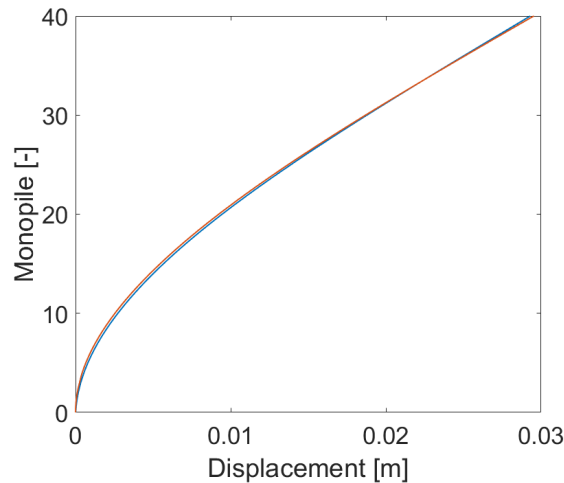


Figure 6.1: Comparison between FD scheme and analytical solution results.

The blue line represents the results of the finite differences scheme and the red line the results of the analytical solution. As it can be observed the two curves are quite close so the finite differences scheme is a good approximation for the calculation of the motions of the spudpoles.

6.2 Connection with the state space model of the vessel

For the calculation of the vessel's motion the forces from the hydraulic cylinder should be calculated. For these forces the relative motions of the vessel and spudpoles should be taken into account. For this reason a general model should be constructed including the state space model of the vessel and a state space model for each spudpole. Four matrices (A,B,C,D) will be constructed for the beam model. In the which will next be added to the vessel model with the procedure which is referred in section 3.5.2. The input in this system will be the wave forces as they are calculated in the chapter 5. The output of the Matlab ode function will contain both the displacements of the vessel and the spudpoles.

The output of the model of the vessel regards only the center of gravity of the vessel. So all the other points of the vessel will have different displacements because of the presence of the three rotations. For this reason the displacements of the connection point of the vessel with the hydraulic cylinders should be calculated for each time step. This can be done by multiplying the displacements of the center of gravity with a transformation matrix which takes into account the three rotations of the vessel.

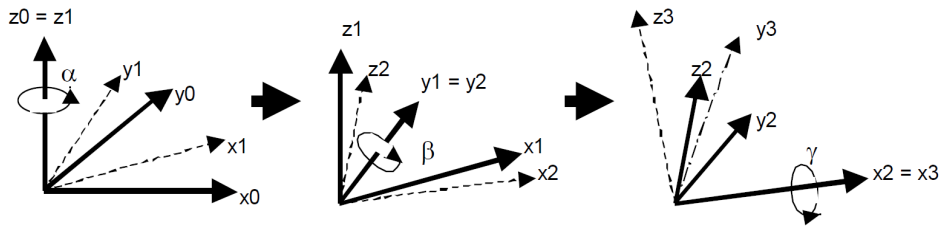


Figure 6.2: Rotation around the three axes.

The displacement of a point because of the rotation of the vessel is an outcome of the summation of the rotations around the three axes. So according to the Figure 6.2 the angle α is the outcome of the yaw motion (around z-axis), the β of the pitch motion (around y-axis) and the γ angle of the roll motion (around x-axis). The total transformation matrix (TTM) is the outcome of the multiplication of the three individual transformation matrices for each angle.

$$\text{TTM} = \begin{bmatrix} \cos(\alpha) & -\sin(\alpha) & 0 \\ \sin(\alpha) & \cos(\alpha) & 0 \\ 0 & 0 & 1 \end{bmatrix} \cdot \begin{bmatrix} \cos(\beta) & 0 & \sin(\beta) \\ 0 & 1 & 0 \\ -\sin(\beta) & 0 & \cos(\beta) \end{bmatrix} \cdot \begin{bmatrix} 1 & 0 & 0 \\ 0 & \cos(\gamma) & -\sin(\gamma) \\ 0 & \sin(\gamma) & \cos(\gamma) \end{bmatrix} \quad (6.4)$$

$$\text{TTM} = \begin{bmatrix} \cos(\alpha)\cos(\beta) & \cos(\alpha)\sin(\beta)\sin(\gamma) - \sin(\alpha)\cos(\gamma) & \cos(\alpha)\sin(\beta)\cos(\gamma) + \sin(\alpha)\sin(\gamma) \\ \sin(\alpha)\cos(\beta) & \sin(\alpha)\sin(\beta)\sin(\gamma) + \cos(\alpha)\cos(\gamma) & \sin(\alpha)\sin(\beta)\cos(\gamma) - \cos(\alpha)\sin(\gamma) \\ -\sin(\beta) & \cos(\beta)\sin(\gamma) & \cos(\beta)\cos(\gamma) \end{bmatrix} \quad (6.5)$$

The 3 by 3 matrix 6.5 is multiplied with the vector of the coordinates of the point of interest. These values are subtracted from the values of the real coordinates. In this way the displacement due to the three angles can be calculated. Consequently the displacements of the center of gravity are added to them and in this way the displacements of every point of the vessel can be found.

So by this way the total model including both the vessel and the poles is constructed. The external forces of this system are the wave forces. Both for the vessel and poles there are the forces from the hydraulic cylinders in the three directions. For a more accurate calculation of these forces the relative motion of the vessel and the spudpoles is taken into account. This relative displacement multiplied by the hydraulic stiffness results in the applied force in the points of interest. Concluding, for each time step the model will calculate the motion of the vessel due to the external wave loads and at the same time the motion of the spudpoles due to the connection to the vessel.

6.3 The lower part of the spudpoles

The lower part of the spudpoles is a suction bucket. A visualization of the suction bucket can be seen in the next Figure.

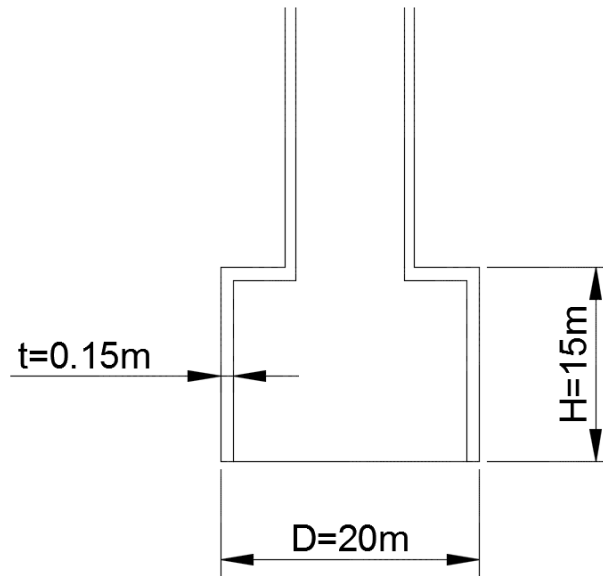


Figure 6.3: Suction bucket dimensions.

The suction bucket of each pole has an outer diameter (D) of 20 meters and a thickness (t) of 15 cm. The penetration depth (H) is 15 meters. So this part will be inserted into the soil for 15 meters and the upper part of the spudpoles will be connected with the vessel.

7 Checks

7.1 Checks for the spudpoles

The spudpoles are steel circular hollow sections. Before the checks a classification check should be performed.

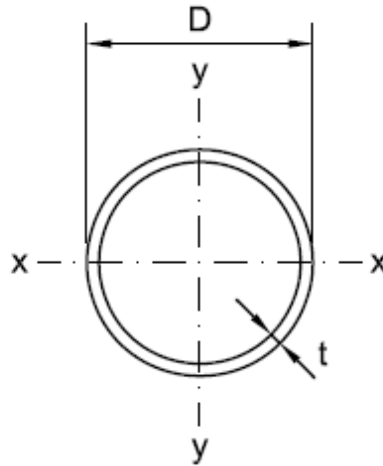


Figure 7.1: Characteristics of a circular hollow section.

The examined spudpoles based on the diameter and the thickness will belong to class 1. This means that the Diameter (D) to thickness (t) ratio is lower than $50 \cdot \epsilon^2$.

$$D/t \leq 50 \cdot \epsilon^2 \quad (7.1)$$

where ϵ is

$$\epsilon = \sqrt{\frac{235}{f_y}} \quad (7.2)$$

with f_y the yield stress of the steel. In this point, it is worth mentioning that a steel with a yield stress of 355 MPa will be used but because of the quite large thickness of the spudpole this number reduces according to the following Table [11]:

The variation of minimum yield strength (N/mm²) with thickness

Steel grade	Nominal thickness (mm)					
	≤ 16	> 16 ≤ 40	> 40 ≤ 63	> 63 ≤ 80	> 80 ≤ 100	> 100 ≤ 150
S275	275	265	255	245	235	225
S355	355	345	335	325	315	295
S420	420	400	390	370	360	340
S460	460	440	430	410	400	380

Figure 7.2: The variation of minimum yield strength with thickness.

So according to the thickness of the hollow section a check should be performed about the real yield stress of the spudpoles.

7.1.1 Stress check

The stress check will be done according to the following equation:

$$\sigma = \frac{N}{A} + \frac{M_y}{W_{el}} + \frac{M_x}{W_{el}} \quad (7.3)$$

Where:

N = Axial force

A = Cross section area

M_y = Moment in y direction

M_x = Moment in z direction

W_{el} = Elastic Modulus

The cross section area and the elastic modulus can be calculated by the following equations:

$$A = \pi \cdot \left(\frac{D}{2}\right)^2 - \pi \cdot \left(\frac{D}{2} - t\right)^2 \quad (7.4)$$

and

$$W_{el} = \pi \cdot \frac{\left(\frac{D}{2}\right)^4 - \left(\frac{D}{2} - t\right)^4}{4 \cdot \frac{D}{2}} \quad (7.5)$$

7.1.2 Global buckling check

As regards the buckling check the following criterion is used according to [12]:

$$\frac{N}{\kappa \cdot N_p} + \frac{\beta_m \cdot M}{M_p} + \Delta n \leq 1 \quad (7.6)$$

Where:

κ = reduction factor for flexural buckling

N_p = plastic compression resistance

β_m = moment coefficient

M_p = plastic resistance moment

Δn = reduced slenderness

Firstly the elastic buckling force N_{kd} and the buckling length s_k should be calculated:

$$N_{kd} = \pi^2 \cdot \frac{EI}{1.1 \cdot s_k^2} \quad (7.7)$$

$$s_k = \beta \cdot L \quad (7.8)$$

For this structure the buckling length coefficient β is 2 because the one end is fixed and the other one is free.

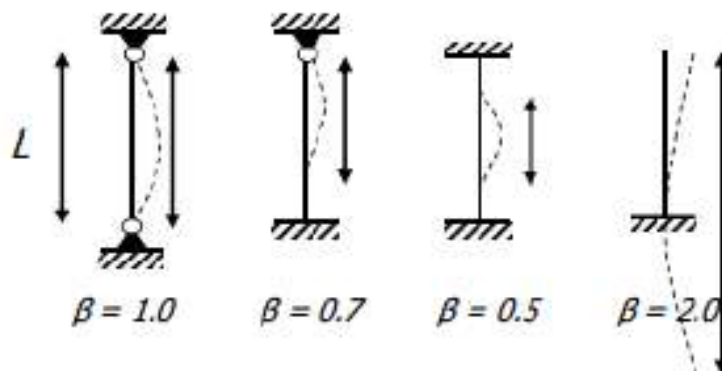


Figure 7.3: Buckling length coefficient.

Next the plastic compression resistance and the plastic moment resistance are calculated:

$$N_p = \frac{A \cdot f_{yield}}{\gamma_m} \quad (7.9)$$

$$M_p = \frac{W_p \cdot f_{yield}}{\gamma_m} \quad (7.10)$$

For the calculation of both a safety factor γ_m of 1.1 is used. The following step is the calculation of the reduced slenderness $\tilde{\lambda}$ and Φ . Where:

$$\tilde{\lambda} = \sqrt{\frac{\gamma_m \cdot N_p}{N_{kd}}} \quad (7.11)$$

and

$$\Phi = 0.5 \cdot (1 + \alpha \cdot (\tilde{\lambda} - 0.2) + \tilde{\lambda}^2) \quad (7.12)$$

For the calculation of the Φ the imperfection factor α should be defined from the following graph. Because of the hollow section the a buckling curve should be used and the α value is equal to 0.21.

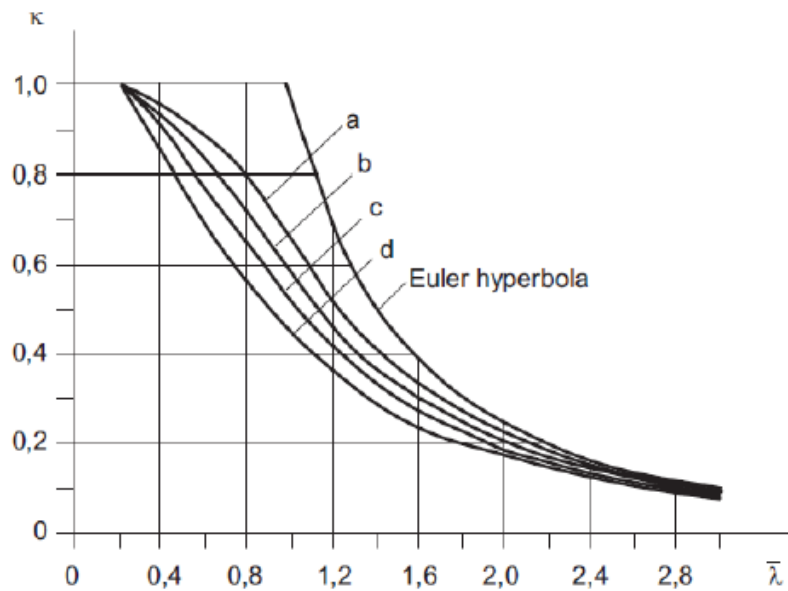


Figure 7.4: Buckling curves a-d.

If the values of Φ and $\tilde{\lambda}$ are known the reduction factor for flexural buckling κ can be calculated according to the following relation:

$$\kappa = \frac{1}{\Phi + \sqrt{\Phi^2 - \tilde{\lambda}^2}}, \text{ for } \tilde{\lambda} > 0.2 \quad (7.13)$$

$$\kappa = 1, \text{ for } \tilde{\lambda} \leq 0.2$$

The reduced slenderness Δn is the minimum value of the $0.25 \cdot \kappa \cdot \tilde{\lambda}^2$ and 0.1. So if the criterion of the equation 7.6 is fulfilled, the structure is safe from buckling problems. In the equation 7.6 the resultant moment M from both directions should be taken into account according to [12]. So

$$M = \sqrt{M_x^2 + M_y^2} \quad (7.14)$$

The stress and the buckling checks are performed at the lower point of the poles (at the seabed). At this point the moments from both the cylinder's and wave forces have the larger value. So this is the critical point of the spudpoles.

7.2 Checks for the suction bucket

The initial design for the suction bucket should be appropriate in order to fulfill all the criteria for the soil checks. Thus the characteristics of the suction bucket are:

- Diameter (D) = 20m
- Thickness (t) = 0.15m
- Depth (H) = 15m

For the whole range of the diameters and thicknesses of the spudpoles the soil check for this suction bucket should be performed in order to ensure that there are not foundation problems.

7.2.1 Pull-out capacity check

Another critical issue is to ensure that the two poles will remain to their positions despite the enormous forces which will be applied on them. For this reason there are some extra checks for the soil structure interaction. As it is described the lower part of the spudpole is a suction bucket which is inserted in the soil with the help of suction. The pull-out capacity check will be performed according to the next equation

$$V = W' + A_{se} \cdot \alpha_e \cdot \tilde{s}_u + A_{si} \cdot \alpha_i \cdot \tilde{s}_u \quad (7.15)$$

Where:

A_{se} = external shaft surface area

A_{si} = internal shaft surface area

α_e = external friction coefficient

α_i = internal friction coefficient

s_u = undrained shear strength

W' = submerged caisson weight

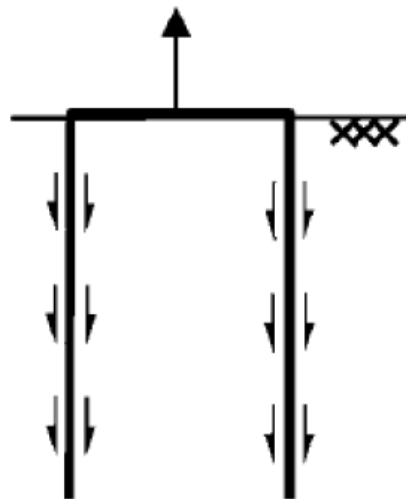


Figure 7.5: External and internal friction forces.

The most common soil type in the North Sea is sand. The caisson is unplugged so both internal and external areas provide friction. The friction coefficient between steel and sand is around 0.3. The undrained shear strength is the integral of the friction force for the whole depth of the caisson.

$$s = \int_0^h \tau_{max} dz \quad (7.16)$$

Where:

$$\tau_{max} = K_o \cdot \gamma' \cdot z \text{ and}$$

K_o = earth pressure coefficient ($K_o = 1 - \tan\phi$)

γ' = effective unit weight

z = depth

ϕ = angle of friction

This is ultimate capacity of the caisson. The final check is the comparison of the axial force with the capacity of the caisson. If the axial tension force is lower than the capacity then the criterion is fulfilled.

7.2.2 Bearing capacity check

The two final checks for the caisson are the bearing capacity checks. One for the vertical and one for the horizontal movement.

The bearing capacity of the caisson in the vertical direction (V') can be calculated from the following relation:

$$V' = \frac{\gamma' \cdot h^2}{2} \cdot K_o \cdot \tan(\delta_o \cdot \pi \cdot D_o) + \frac{\gamma' \cdot h^2}{2} \cdot K_o \cdot \tan(\delta_i \cdot \pi \cdot D_i) + (\gamma' \cdot h \cdot N_q + \gamma' \cdot \frac{t}{2} N_\gamma) \quad (7.17)$$

Where:

δ = soil/wall friction angle

D_o = outer diameter

D_i = inner diameter

N_γ = drained soil-weight capacity factor

N_q = drained overburden capacity factor

The bearing capacity factors N_γ and N_q are dependent on the angle of friction of the sand and they can be calculated according to the [13]. So the final check will be:

$$V + W_{pole} < V' \quad (7.18)$$

Where:

V = vertical force from the system

W_{pole} = the weight of the pole

As regards the horizontal bearing capacity, it can be calculated based on the next equation:

$$H' = D_o \cdot \int_0^h K_p \cdot \gamma' \cdot z dz - D_o \cdot \int_0^h K_a \cdot \gamma' \cdot z dz \quad (7.19)$$

Where:

K_p = passive earth pressure coefficient

K_a = active earth pressure coefficient

These two coefficients are related to each other with the following formula:

$$K_p = \frac{1}{K_a} = \frac{1 + \tan\phi}{1 - \tan\phi} \quad (7.20)$$

This is the horizontal bearing capacity of the caisson and it should be compared with the resultant horizontal force from the motions of the system. The resultant force will be the square root of the squares of the two horizontal forces in x and y direction.



8 Results

After the construction of the total model (including both the vessel and the two spudpoles) and the calculation of the wave forces, the next step is the performance of simulations in order to observe the motions of the vessel in relation with the wave forces and the presence of the spudpoles. The duration of each simulation is defined in 3 hours. The reason for this decision is because a 3 hour simulation is the minimum in order to consider a full irregular sea state. As it is described in Chapter 6 the provided values from WAMIT are for 13 directions of the wave from 0° to 180° every 15° because of the symmetry of the vessel. The two main parameters which will be examined in these simulations are the diameter and the thickness of the spudpoles in order to find an optimum design for them. For each set of diameter and thickness all the wave directions should be taken into account in order to perform all the necessary checks. Of course except for the stability and the soil checks there is also a check about the motions of the vessel which is the key point of this assignment. There are some limits about the motions of the vessel. The roll angle should be less than 2.5° in order to avoid collision between the transition piece and the substructure during the installation procedure. Also the sway and surge motions should be less than 0.3-0.4m for better accuracy during the installation. These values are the optimum values which will be achieved with the use of Dynamic Positioning System (DPS). So these values are a realistic target to be achieved.

The last step before the start of the simulation is the definition of the initial conditions. Because it is not possible a vessel in the open sea to have zero initial conditions it will be a very rough approximation to consider zero initial conditions. One solution is to run the model for a specific time (some minutes) and then use the output of this simulation as initial conditions of the real 3 hours simulation. By this way it is possible to create a more realistic model of the vessel in a random sea.

Lastly there are some parameters which will be the same for all the sets of the simulation. The depth of the water is 30m and the draft of the vessel is around 7.5m. The total length of the piles is 40m from the seabed (without taking into consideration the suction buckets). Also all the simulations will be run for a wave height of 2.5m with a peak period of 13s.

8.1 Simulation for the initial design

The values of the parameters for the first simulation are 8m for the diameter and 0.4m for thickness. In the next Figures the motions of the vessel in the six degrees of freedom and the motions of the spudpoles in both x and y - direction can be observed.

8.1.1 Motions of the vessel

In the following Figure the motions of the vessel for the 6 degrees of freedom are shown for a simulation period of 400sec (for better visualization). These specific Figures show the motions of the vessel for the wave direction of 105° . This direction is the most critical for the displacements and the rotations of the vessel.

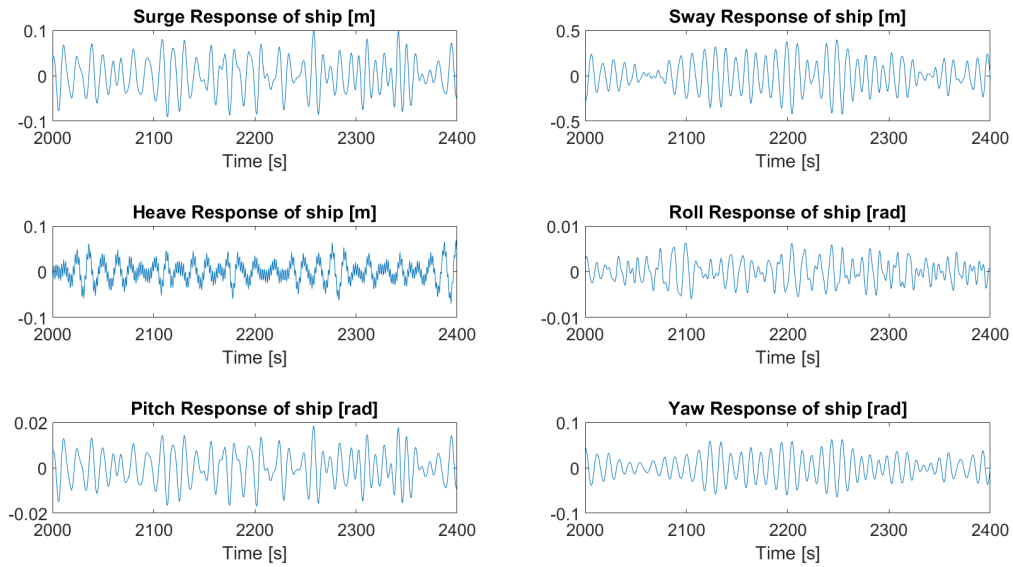


Figure 8.1: The 6 motions of the vessel for a simulation of 400sec ($D=8m$ and $t=0.4m$).

As it was observed from the simulations the two most critical cases are the wave directions 105° and 135° . The maximum values of each motion of the vessel for both wave directions can be seen in the next Table.

	Direction 105°	Direction 135°
Surge (m)	0.1195	0.1279
Sway (m)	0.4152	0.3302
Heave (m)	0.0916	0.0647
Pitch ($^\circ$)	0.3953	0.2922
Roll ($^\circ$)	1.2261	1.3123
Yaw ($^\circ$)	3.6800	2.8533

Table 8.1: Maximum values of the 6 motions of the vessel.

8.1.2 Motion of the spudpoles

In the Figure 8.2 the motions of the spudpoles (left and right) in the x and y direction are shown for the wave direction 105° , during the same simulation period of 400sec.

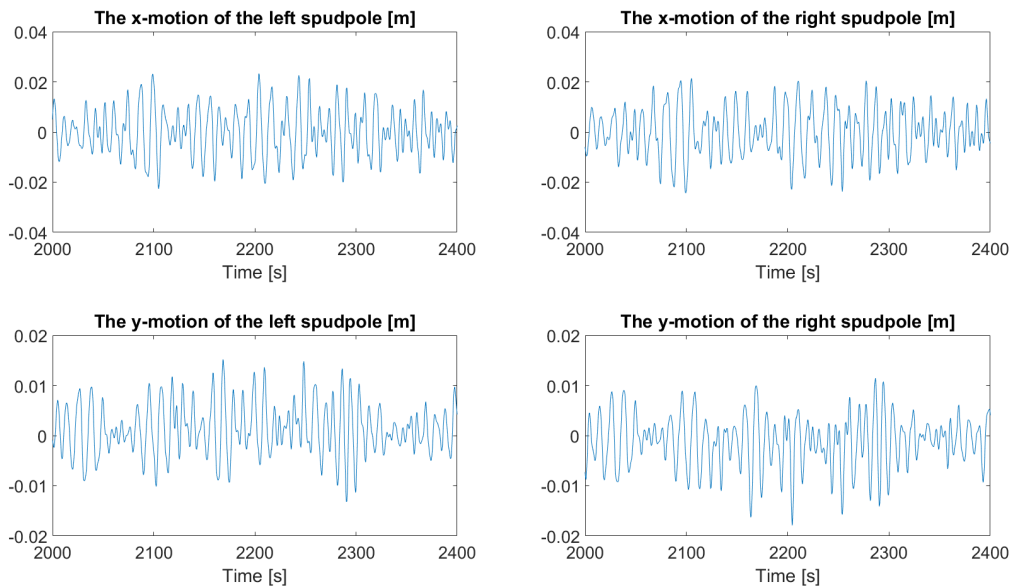


Figure 8.2: The motions of the spudpoles in x and y direction for a simulation of 400sec ($D=8m$ and $t=0.4m$).

The largest values of the displacement of the poles in both directions are shown in the next Table.

	Maximum displacement in x-direction (m)	Maximum displacement in y-direction (m)
Right spudpole	0.0256	0.0166
Left spudpole	0.0266	0.0121

Table 8.2: Maximum values of the displacement of the spudpoles.

8.1.3 Checks

The first check about the range of the motions of the vessel is fulfilled since the vessel has displacements and rotations according to the desirable limits. The next step is the checks about the structure itself as well as the soil structure interaction. The results for the checks for the critical wave directions are shown in the following Table.

	Direction 105°	Direction 135°
Stress check (MPa)	266.54	251.76
Buckling check (-)	0.4825	0.2459
Pull-out check (MN)	24.838	16.407
Bearing capacity check (Horizontal) (MN)	112.73	91.558
Bearing capacity check (Vertical) (MN)	45.360	34.126
Axial tension check (MN)	34.838	16.407

Table 8.3: Maximum values of the checks.

It is worth mentioning that those 2 wave directions are the critical for the stress checks. All the other criteria are fulfilled quite easily for all the other wave directions.

8.2 Extra tests for optimization

After the initial guess some extra simulations will be run in order to optimize the design of the spudpoles. According to the results of the first simulations the critical wave directions are the 105° and 135° . So in order to reduce the simulation time the next tests will be performed only for those 2 directions. These 2 directions are shown with a red arrow in the next Figure.

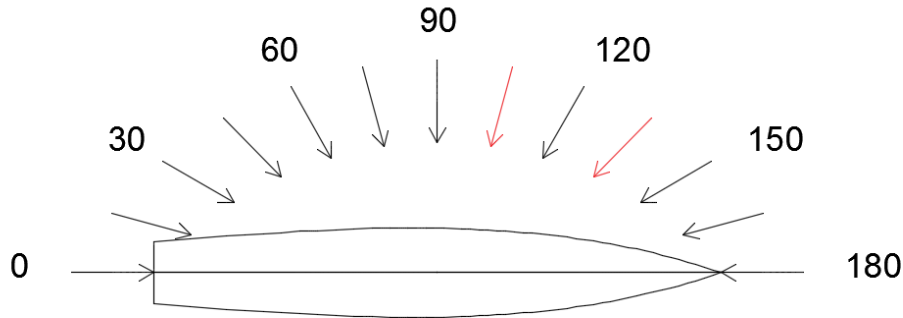


Figure 8.3: Critical wave directions.

The extra tests have the following combinations of diameter and thickness.

Test ID	Diameter (m)	Thickness (m)	Result
Test 1	8	0.35	Failed
Test 3	9	0.3	Good
Test 5	10	0.25	Good

Table 8.4: Test parameters and results for steel type S355.

After those tests, the result was that with this specific type of steel (S355) a quite thick structure is needed. This has multiple disadvantages such as the heavy weight of the structure and a complex design. Also the welding is quite difficult for this thickness and the structure should be casted. In order to avoid these problems it was decided a change in the type of steel from S355 to S690. This type of steel is more expensive but the structure will be lighter. So a new set of simulations will be run. The combination of diameter and thickness for the next set as well as the outcome are presented in the following Table.

Test ID	Diameter (m)	Thickness (m)	Result
Test 2	9.5	0.09	Failed
Test 4	10	0.09	Failed
Test 1	11	0.09	Failed
Test 5	11	0.10	Good

Table 8.5: Test parameters and results for steel type S690.

After the completion of the second set of simulations using the new type of steel, all the tests are plotted in the following Figure.

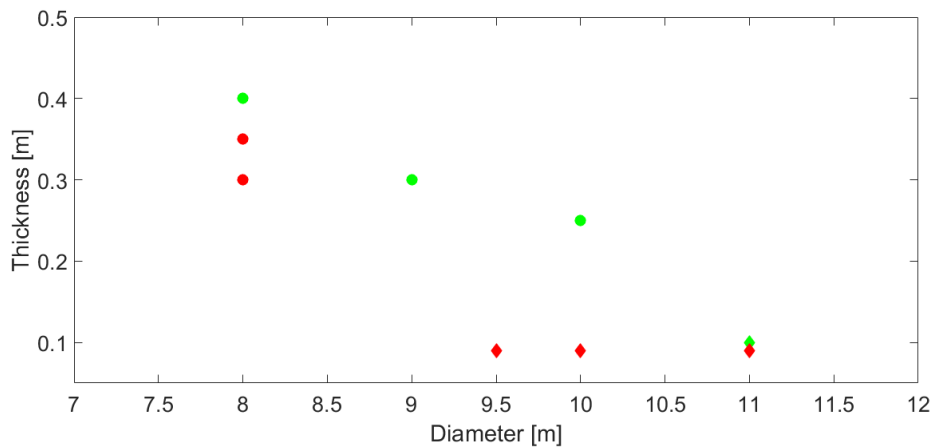


Figure 8.4: Test results.

The dots with the circle shape describe the tests with S355 steel and those with the diamond shape show the tests with S690 steel. The tests which passed all the checks are indicated with green color and the tests which have failed in one or more tests are indicated with red color. As it can be observed the best combination of weight and strength of the structure is the set with a 11m diameter and a thickness of 0.10m.

8.3 The optimum design

8.3.1 Motion of the vessel

As it is described above the optimum design for the spudpoles is a pole with diameter of 11m and a thickness of 0.10m. The motions of the vessel for a 400sec simulation for the wave direction of 105° are shown in the next Figure.

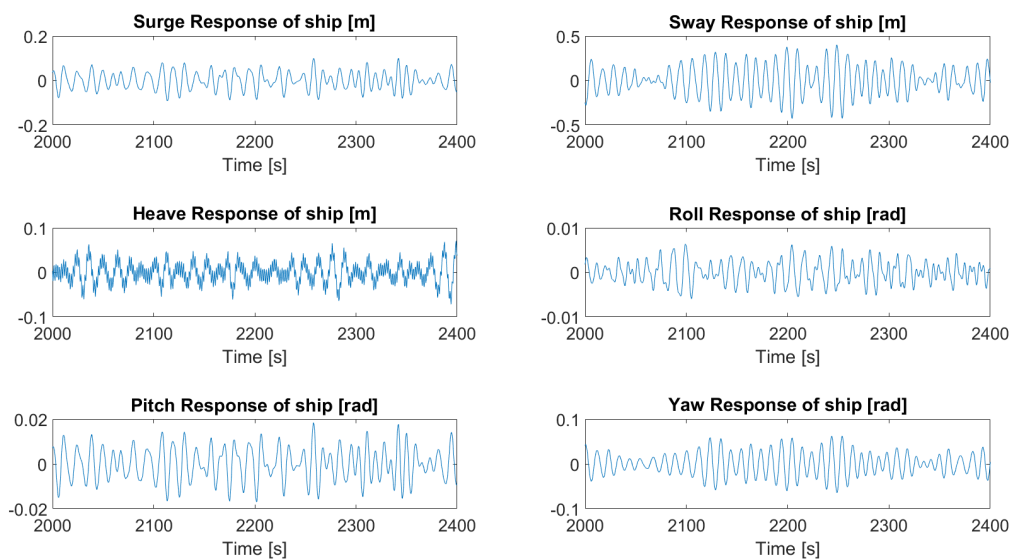


Figure 8.5: The 6 motion of the vessel for 400sec simulation (D=11m and t=0.10m).

The maximum values for each motion can be seen in the following Table.

Direction 105°	
Surge (m)	0.1209
Sway (m)	0.3876
Heave (m)	0.0924
Pitch (°)	0.3951
Roll (°)	1.2360
Yaw (°)	3.6200

Table 8.6: Maximum values of the 6 motions of the vessel.

8.3.2 Motion of the spudpoles

In the next Figures the motions of the spudpoles in the x and y direction are shown for the wave direction of 105° for a simulation period of 400sec.

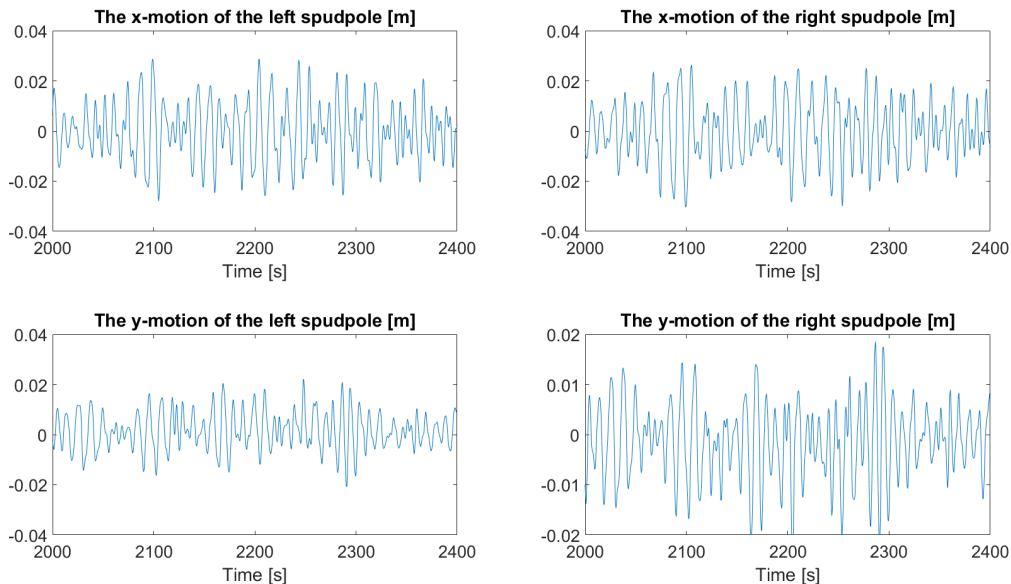


Figure 8.6: The motions of the spudpoles in x and y direction for a simulation of 400sec ($D=11m$ and $t=0.10m$).

The maximum values of the displacements of the two poles in both directions can be seen in the following Table.

	Maximum displacement in x-direction (m)	Maximum displacement in y-direction (m)
Right spudpole	0.0320	0.0234
Left spudpole	0.0325	0.0203

Table 8.7: Maximum values of the displacement of the spudpoles.

8.3.3 Final Checks

From the whole range of the simulations it was observed that the wave direction of 90° is the worst for the pull-out capacity because this wave is perpendicular to the vessel. For the same reason also this wave direction is also checked for the final design. The motion of the 6 degrees of freedom of the vessel and the displacements of the spudpoles for this wave direction are shown in the following Figures. For better

visualization only a small part of the whole 3 hrs simulation is shown. The whole simulation can be found in Appendix C.

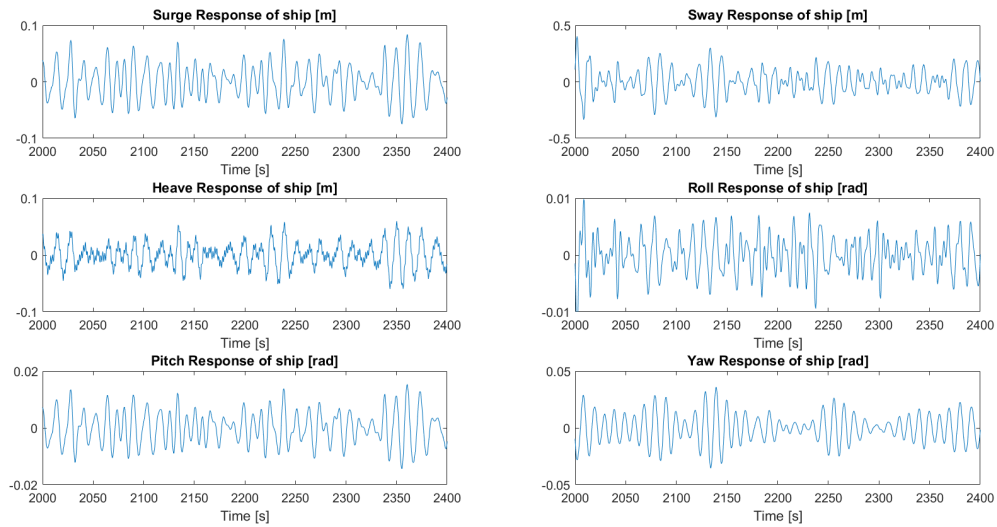


Figure 8.7: The 6 motions of the vessel for a simulation of 400sec ($D=11m$ and $t=0.10m$).

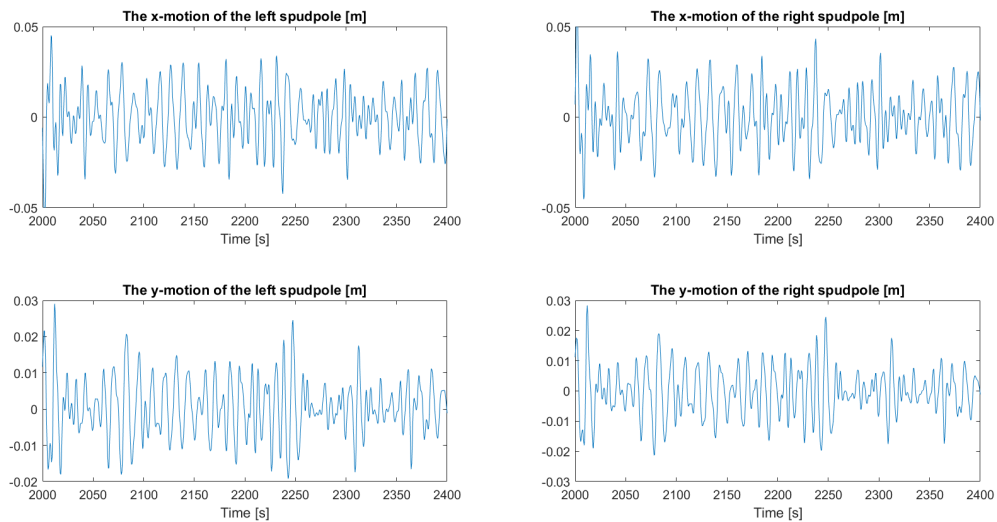


Figure 8.8: The motions of the spudpoles in x and y direction for a simulation of 400sec ($D=11m$ and $t=0.10m$).

The results for the checks for the wave directions of 90° and 105° are shown in the next Table.



	Direction 90°	Direction 105°	Limit
Stress check (MPa)	541.59	561.30	590.00
Buckling check (-)	0.8189	0.8188	1.0000
Pull-out check (MN)	23.365	18.274	25.000
Bearing capacity check (Horizontal) (MN)	108.088	113.36	147.70
Bearing capacity check (Vertical) (MN)	29.728	39.370	74.767
Axial tension check (MN)	18.274	23.365	1502.3

Table 8.8: Maximum values of the checks.

So this specific design of the spudpoles is proven sufficient to reduce the motions of the vessel and makes possible to keep the vessel within the desirable limits. This specific set of 11m diameter and 0.10 m thickness is strong enough in order to fulfill all the necessary criteria. Moreover the design of the suction bucket at the lower end of the spudpoles makes the whole substructure stable despite the huge forces and moments achieving the initial goal.

9 Conclusions and Recommendations

In this chapter a summary will be given about the steps which were followed in this project. The results are discussed in section 9.2. Furthermore the recommendations and the contributions to the project are presented.

9.1 Summary

In chapter 2, the alternatives about the foundation types were discussed. A MCA was performed for spudpoles with conical end, monopiles with vibrating hammer and spudpoles with suction buckets. The suction buckets were the best choice for this specific project.

In the following chapter, a model for the vessel has been created in Matlab. For the construction of the model a state space model was used instead of the convolution scheme in order to reduce the computational time. In order to validate the state space model (approximation system), the results of this model were compared with the results of another Matlab model based on the convolution scheme. The compensation system and the whole installation procedure were analyzed in Chapter 4.

In Chapter 5, a model for an irregular sea state was made based on the superposition principle. In Chapter 6 the final model was created containing both the vessel, the spudpoles and the environmental forces. In the last Chapter, the final checks were performed in order to check the strength and the stability of the structure and its interaction with the soil.

9.2 Results Analysis

The main outcome of the results is that this idea is a realistic and feasible solution. It is a goal that can be achieved and maybe become a new way of motion compensation of the vessels. Certainly there is room for improvement but as it can be seen from the results, the displacements and rotations of the vessel are between the allowable limits and comparable with them using the Dynamic Positioning Systems. Moreover, the values of the diameter and thickness of the spudpoles are quite large but they are in a logical order of magnitude.

Furthermore, the design with the suction buckets was the best choice for this project because this way the spudpoles can be inserted and extracted in a relatively easy and quick way. By selecting this particular concept, the two cranes of the vessel remain free to install the transition pieces so the whole installation procedure becomes less time consuming.

Looking at the results specifically, the optimum design of the spudpoles, which was one of the main goals of this project, is a set with 11 *m* diameter and 0.10 *m* thickness constructed by steel S690. The maximum displacement is around 40 *cm* in sway direction and the maximum rotation is about 3° in the yaw motion.

The results were examined in more detailed way and some facts about the wave directions and the vessel came out. The wave directions of 105° and 135° were the most critical for the stress and the buckling checks. On the other hand the wave direction of the 90° was the most critical regarding the pull-out capacity check since the waves in this case are perpendicular to the vessel. These three wave directions should be avoided if it is possible with the correct placing of the vessel. The whole compensation system is designed in order to withstand those conditions but it is preferable to avoid them for several issues such as fatigue problems. I

It was also observed that the spudpoles have relatively small displacements in both directions (x and y). The displacements are around 4-5 *cm*.



9.3 Recommendations

It is worth mentioning that the above results are based on a set of assumptions. Therefore, it should be remarked that the present research not only describes a way of motion compensation of the vessel but it also gives rise to further research and investigation in order to create a more detailed model. In order to improve the model, the following recommendations are suggested.

In the present research the boundary conditions were a free end for the upper end and a fix end for the lower end. A better approach of the boundary conditions will result to a more accurate outcome. The lower end can be considered as a free end and the soil can be modeled as springs which retain the lower end stable. By this way a better representation of the reality can be achieved.

Moreover, a more detailed analysis and examination of the soil properties should be performed. Due to the cycling loading, the soil-structure interaction should be examined quite accurately. Furthermore, phenomena such as liquefaction should be checked carefully because they are quite common on offshore structures.

Another part which will need extra research is the mechanical system of the compensation system. This system will be designed to carry and lift quite heavy structures, so a detailed design of the control system is a necessity for safety reasons.

Furthermore, for this project a basic assumption is that the vessel is modeled as a rigid body. With a finite elements program a better representation of real conditions could be achieved since a more accurate vessel model can be constructed.

Moreover, some real scale tests in a basin will definitely help towards the validation of the state space model. There will again be some doubts about the soil properties but the results can show if the model could be used in real life.

Lastly, a cost analysis is necessary in order to compare this compensation system with the Dynamic Positioning Systems (DPS). The cost of the construction and the operation with the compensation system should be less than the DPS. Otherwise a change and an optimization of the design is needed.

9.4 Contributions of this project

The first contribution of this project is the research about the reduction of the vessel movements using a compensation system. Compensation systems are used and especially in the offshore industry in access bridges or in grippers but not for the stabilization of a vessel. Moreover, the idea with the spudpoles has begun from the cutter suction dredger vessels. But those vessels operate in ports without large wave heights.

The vessel model created for this project can also be considered as a contribution. This Matlab model can read the inputs from a WAMIT file and it can calculate the motions of the vessel for specific environmental loads. The model is also constructed in the time domain so it can handle any possible non-linearity. Lastly some extra aspects such as mooring lines can easily be inserted to the model following the same procedure.

References

- [1] Prof.Ir. W.J.Vlasblom. *Designing Dredging equipment*. May 2003.
- [2] Van Aalst Bulk Handling B.V.. *Spud poles solution*. February 2013.
- [3] PVE piling and vibro equipment. *Offshore vibratory hammers product range*. 2016.
- [4] WAMIT INC. *Wamit user manual*. 2006.
- [5] J.M.J Journee AND W.W Massie. *Offshore Hydromechanics*. 2001.
- [6] A.V.Metrikine. *Dynamics, Slender Structures and an Introduction to Continuum Mechanics*. 2016.
- [7] Eugene L.Duke. *Combining and Connecting Linear,Multi-Input,Multi-Output Subsystem Models*. April 1986.
- [8] Peter Albers. *Motion Control in Offshore and Dredging*. 2010.
- [9] Leo H.Holthijzen. *Waves in Oceanic and Coastal Waters*. 2007.
- [10] Chris Kijdener and Antonio Jarquin-Laguna. *Introduction to Computational Dynamics of Offshore Structures (Lectures)*. 2016.
- [11] European committee for standardization. *Eurocode 3: Design of steel structures- Part 1-1: General rules and rules for buildings*. 2003.
- [12] *GL Guideline for the Certification of Offshore Wind Turbines*. 2005.
- [13] Braja M. Das. *Fundamentals of Geotechnical Engineering*. 2005.



Appendix A JUMBO KINETIC Specifications



K3000 Class HLV Jumbo Kinetic

Port of registry:	Rotterdam
Flag:	Netherlands
Classification:	Lloyd's Register +100 A1 strengthened for heavy cargoes +LMC, UMS, CG, LI, IWS, Ice Class 1A Finnish Swedish
General agent:	Kahn Scheepvaart B.V. Rotterdam
Ice Class:	1A Finnish Swedish
Deadweight (summer) abt:	14,000 T
Draft (above bottom of keel):	8.1 m
Length o.a.:	152.60 m
Beam moulded:	27.4 m
Free deck space:	3,250 m ²
No. of holds:	1
No. of hatches:	1
Bale capacity:	20,868 m ³ (with tweendecks fitted)
Hold: dimensions lower hold:	83.2 x 17.0 x 5.6 m
Hold: dimensions upper hold:	108.8 x 17.0 x 7.0 m
Hold: total height:	12.6 m
Strength of tanktop:	12 T/m ²
Strength of tweendecks:	7 T/m ²
Strength of hatchcovers:	6 x 8.7 T/m ² and 3 x 12 T/m ²
No. of tweendecks:	1 (flush) adjustable in height
Cargo gear:	2 x 1,500 T mastcrane, combinable to 3,000 T
Main engine(s):	2 x CPP/ME with MAK 9M32G engines, total of 9,000 kW
Thruster(s):	Bowthruster: Berg - 1,500 kW
Speed:	17.00 knots

This new vessel, which represents the latest evolutionary step in the Jumbo fleet is both larger and stronger than its predecessors. It has a dual lift capability of up to 3,000t and it is certified Ice Class 1A Swedish/Finnish for extra versatility. Jumbo Kinetic is one of the two vessels from the K-class family. Fitted with two 1,500t crane with a combined lift capacity of 3,000t.

Appendix B Finite differences scheme

As it is previously discussed the beam is discretized with the help of the finite differences scheme. If the beam is discretized in N nodes (so $N-1$ elements) and it has length L , the length of each element is

$$l = \frac{L}{N-1}.$$

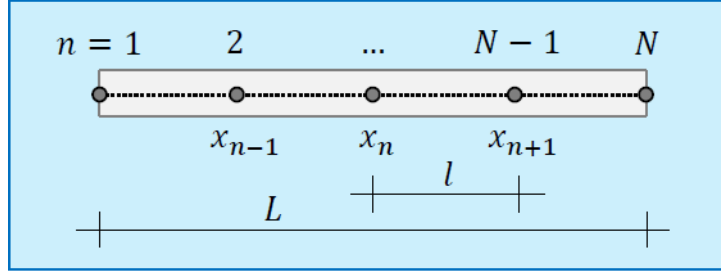


Figure B.1: Discretization of a beam

The equation of the beam is

$$EI \cdot w''''(x, t) + \rho \cdot A \cdot \ddot{w}(x, t) = F \quad (\text{B.1})$$

With the use of the finite differences scheme the term $w''''(x_n)$ will be replaced by the displacements of the points around the specific point. Analytically the Taylor Series Expansion (TSE) will be evaluated at x_n and 2 points at the left side and two points on the right, because the order of this term is 4. The distance between the points is

$$(x_{n+2} - x_n) = 2 \cdot l, (x_{n+1} - x_n) = l, (x_{n-1} - x_n) = -l, (x_{n-2} - x_n) = -2 \cdot l \quad (\text{B.2})$$

The TSE for the five points are the following:

$$w(x_{n+2}) = w(x_n) + 2 \cdot l \cdot w'(x_n) + 4 \cdot \frac{l^2}{2} \cdot w''(x_n) + 8 \cdot \frac{l^3}{6} \cdot w'''(x_n) + 16 \cdot \frac{l^4}{24} \cdot w''''(x_n) \quad (\text{B.3})$$

$$w(x_{n+1}) = w(x_n) + l \cdot w'(x_n) + \frac{l^2}{2} \cdot w''(x_n) + \frac{l^3}{6} \cdot w'''(x_n) + \frac{l^4}{24} \cdot w''''(x_n) \quad (\text{B.4})$$

$$w(x_n) = w(x_n) \quad (\text{B.5})$$

$$w(x_{n-1}) = w(x_n) - l \cdot w'(x_n) + \frac{l^2}{2} \cdot w''(x_n) - \frac{l^3}{6} \cdot w'''(x_n) + \frac{l^4}{24} \cdot w''''(x_n) \quad (\text{B.6})$$

$$w(x_{n-2}) = w(x_n) - 2 \cdot l \cdot w'(x_n) + 4 \cdot \frac{l^2}{2} \cdot w''(x_n) - 8 \cdot \frac{l^3}{6} \cdot w'''(x_n) + 16 \cdot \frac{l^4}{24} \cdot w''''(x_n) \quad (\text{B.7})$$

The next step is to find a way to sum these 5 evaluations in such a way that only the $w''''(x_n)$ remains:

$$\alpha \cdot w(x_{n-2}) + \beta \cdot w(x_{n-1}) + \gamma \cdot w(x_n) + \delta \cdot w(x_{n+1}) + \epsilon \cdot w(x_{n+2}) = w''''(x_n) + \text{error} \quad (\text{B.8})$$

There are 5 equations and 5 unknown coefficients, so solving the following system the 5 unknown can be easily found.

$$\begin{bmatrix} 1 & 1 & 1 & 1 & 1 \\ 2l & l & 0 & -l & -2l \\ 2l^2 & \frac{l^2}{2} & 0 & \frac{l^2}{2} & 2l^2 \\ \frac{8l^3}{6} & \frac{l^3}{6} & 0 & -\frac{l^3}{6} & -\frac{8l^3}{6} \\ \frac{6}{16l^4} & \frac{6}{l^4} & 0 & \frac{6}{l^4} & \frac{6}{16l^4} \\ \frac{1}{24} & \frac{1}{24} & 0 & \frac{1}{24} & \frac{1}{24} \end{bmatrix} \cdot \begin{bmatrix} \alpha \\ \beta \\ \gamma \\ \delta \\ \epsilon \end{bmatrix} = \begin{bmatrix} 0 \\ 0 \\ 0 \\ 0 \\ 0 \\ 0 \end{bmatrix} \quad (\text{B.9})$$

Since the 5 coefficients are now known the term $w''''(x_n)$ can be calculated by the next formula:

$$w''''(x_n) = \frac{w(x_{n-2}) - 4 \cdot w(x_{n-1}) + 6 \cdot w(x_n) - 4 \cdot w(x_{n+1}) + w(x_{n+2}))}{l^4} \quad (\text{B.10})$$

For the evaluation of the TSE there is a need for 2 points on the left of the forepart of the beam as well as 2 points on the right of the end of the beam which are not on the beam and they should be replaced. In order to achieve this the next step is the application of the boundary conditions. As it is discussed the bottom end is fixed and the top one is free. Following the same procedure these points can be replaced by the above equations (for an example with N=7 points):

$$w_1 = 0 \rightarrow \quad (\text{B.11})$$

$$w'_1 = 0 \rightarrow w_{-1} = w_3 \quad (\text{B.12})$$

$$w'_7 = 0 \rightarrow 2 \cdot w_8 = w_7 - w_6 \quad (\text{B.13})$$

$$EI \cdot w''_7 = -F \rightarrow w_9 = \frac{2l^3 F}{EI} + w_5 - 4w_6 + 4w_7 \quad (\text{B.14})$$

Applying the above boundary conditions the final equation of motion for a beam with 7 nodes and a fixed and a free end is reached.

$$\rho \cdot A \cdot \begin{bmatrix} 1 & 0 & 0 & 0 & 0 & 0 \\ 0 & 1 & 0 & 0 & 0 & 0 \\ 0 & 0 & 1 & 0 & 0 & 0 \\ 0 & 0 & 0 & 1 & 0 & 0 \\ 0 & 0 & 0 & 0 & 1 & 0 \\ 0 & 0 & 0 & 0 & 0 & 1 \end{bmatrix} \cdot \begin{bmatrix} \ddot{w}_2 \\ \ddot{w}_3 \\ \ddot{w}_4 \\ \ddot{w}_5 \\ \ddot{w}_6 \\ \ddot{w}_7 \end{bmatrix} + \frac{EI}{l^4} \cdot \begin{bmatrix} 7 & -4 & 1 & 0 & 0 & 0 \\ -4 & 6 & -4 & 1 & 0 & 0 \\ 1 & -4 & 6 & -4 & 1 & 0 \\ 0 & 1 & -4 & 6 & -4 & 1 \\ 0 & 0 & 1 & -4 & 5 & -2 \\ 0 & 0 & 0 & 2 & -4 & 2 \end{bmatrix} \cdot \begin{bmatrix} w_2 \\ w_3 \\ w_4 \\ w_5 \\ w_6 \\ w_7 \end{bmatrix} = \begin{bmatrix} F_2 \\ F_3 \\ F_4 \\ F_5 \\ F_6 \\ F_7 \end{bmatrix} \quad (\text{B.15})$$

Appendix C Motions of the vessel

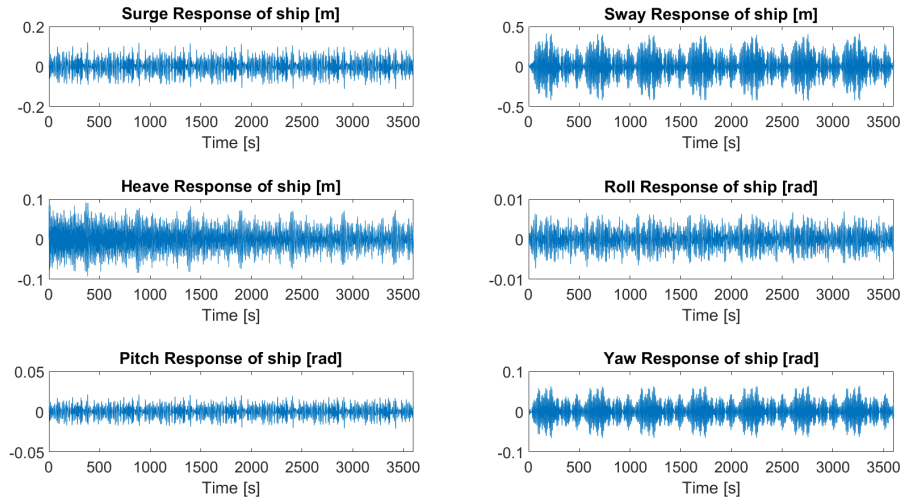


Figure C.1: The 6 motion of the vessel ($D=8m, t=0.35m$, Wave direction 105°).

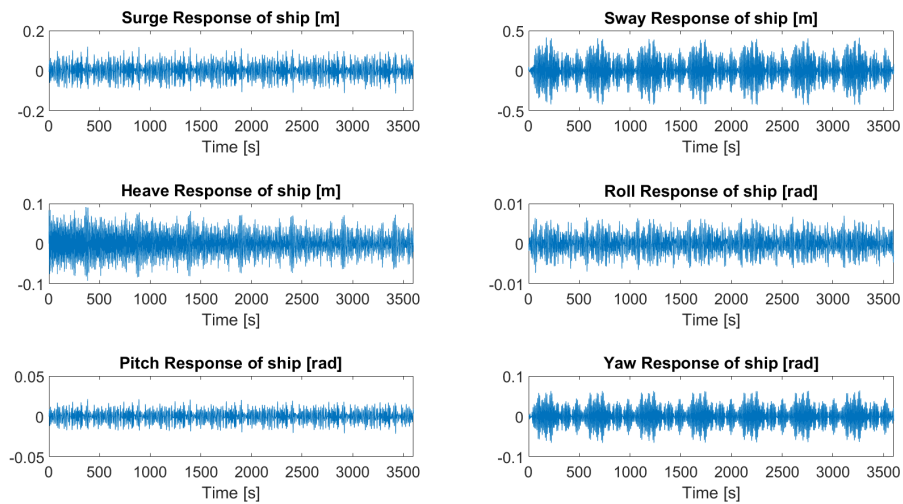


Figure C.2: The 6 motion of the vessel ($D=8m, t=0.40m$, Wave direction 105°).

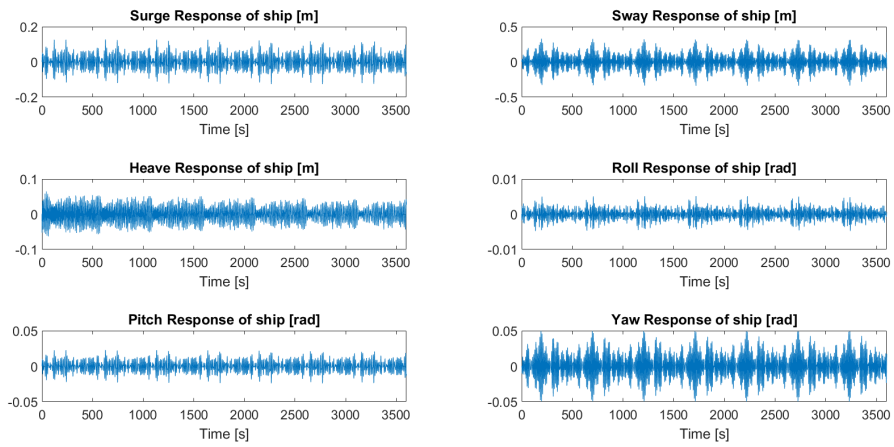


Figure C.3: The 6 motion of the vessel ($D=8m, t=0.40m$, Wave direction 135°).

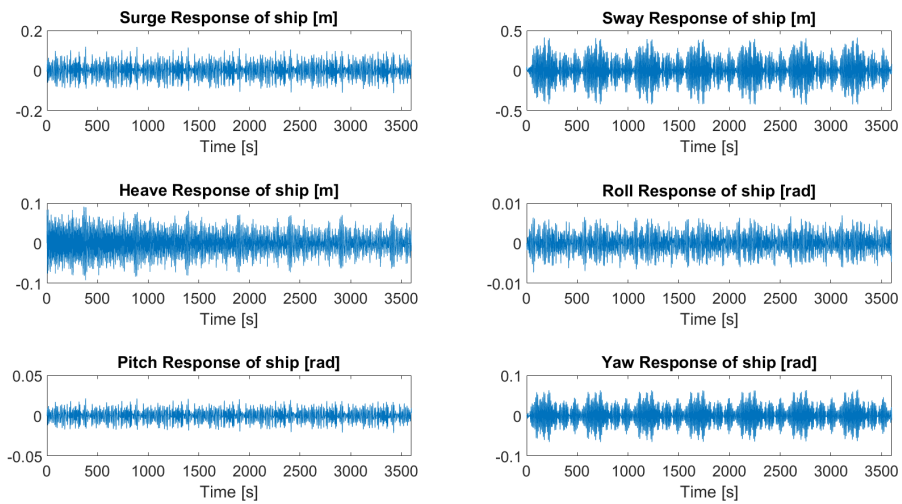


Figure C.4: The 6 motion of the vessel ($D=9m, t=0.30m$, Wave direction 105°).

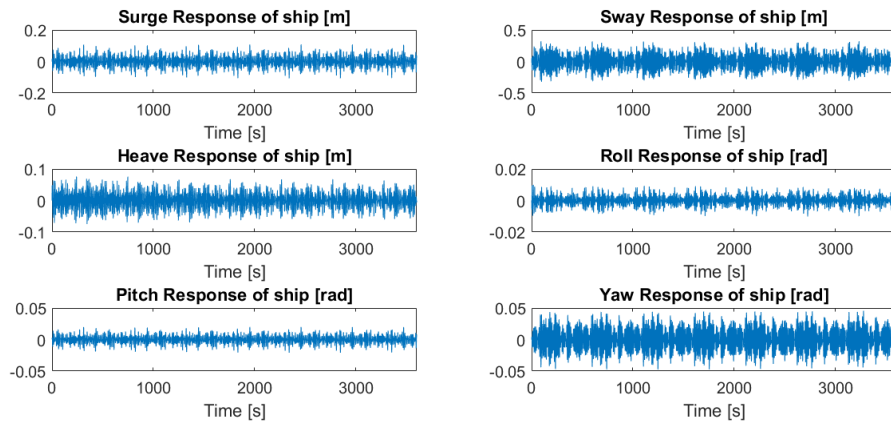


Figure C.5: The 6 motion of the vessel ($D=9.5m, t=0.09m$, Wave direction 105°).

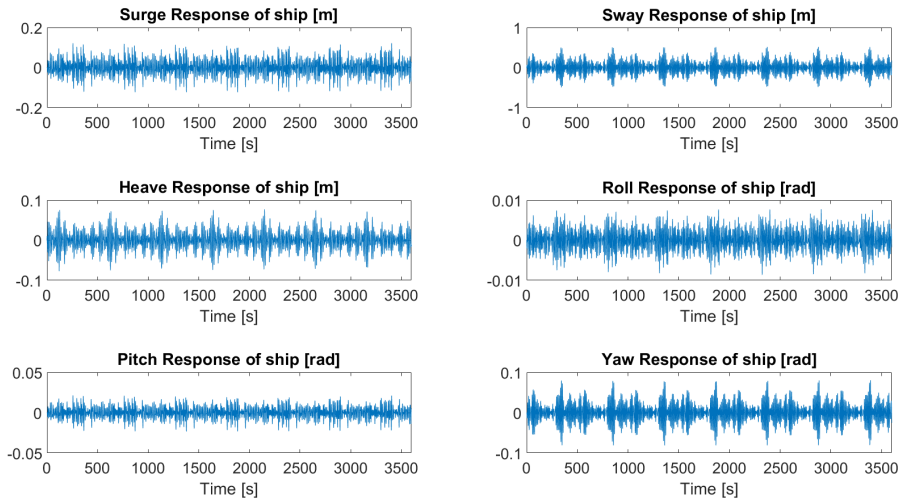


Figure C.6: The 6 motion of the vessel ($D=10m, t=0.09m$, Wave direction 105°).

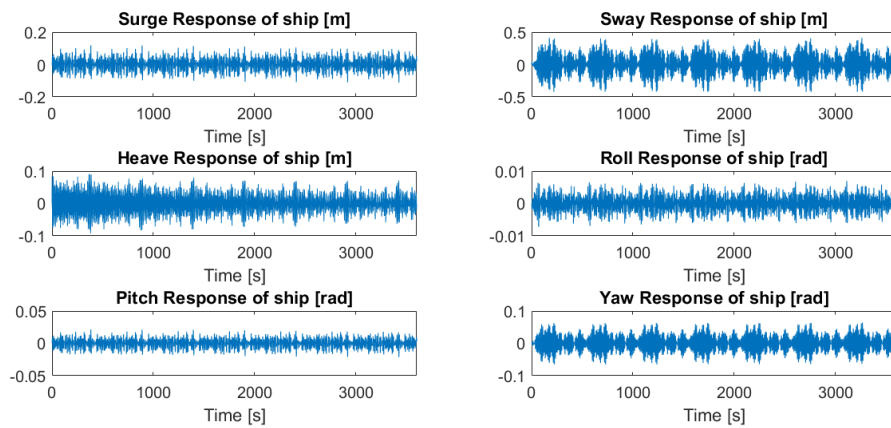


Figure C.7: The 6 motion of the vessel ($D=10m, t=0.25m$, Wave direction 105°).

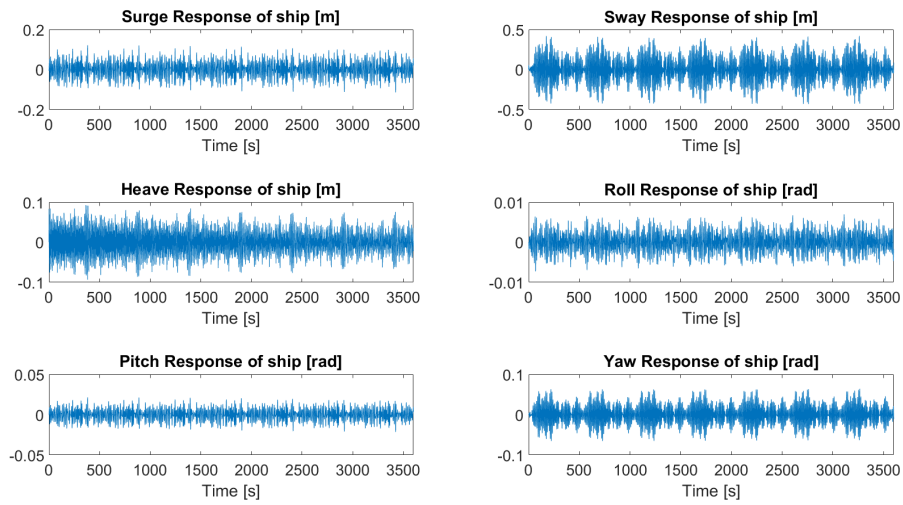


Figure C.8: The 6 motion of the vessel ($D=11m, t=0.09m$, Wave direction 105°).

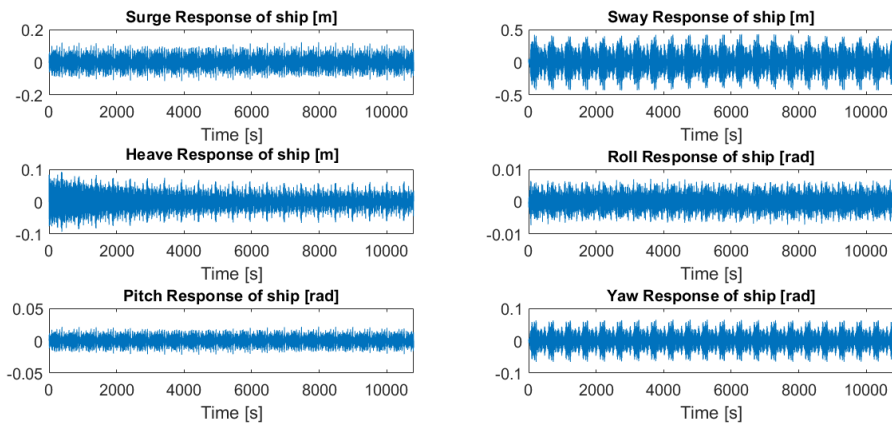


Figure C.9: The 6 motion of the vessel ($D=11m, t=0.10m$, Wave direction 105°).

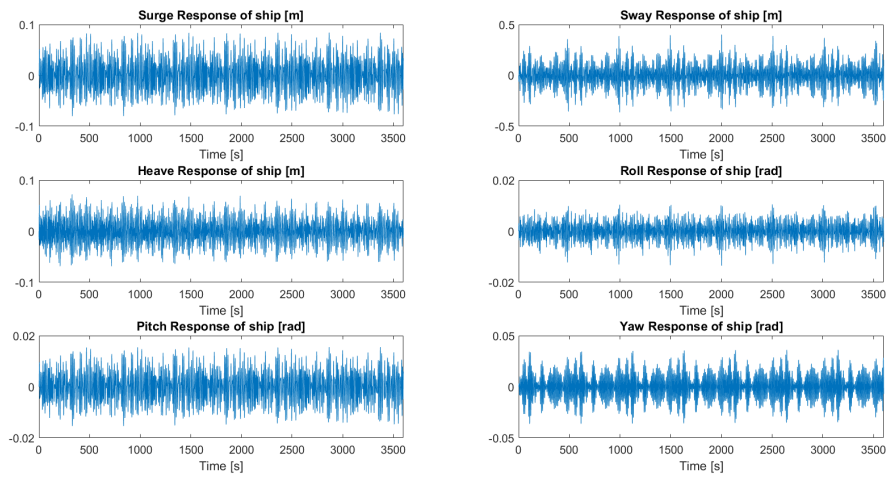


Figure C.10: The 6 motion of the vessel ($D=11m, t=0.10m, \text{Wave direction } 90^\circ$).

Appendix D Motions of the spudpoles

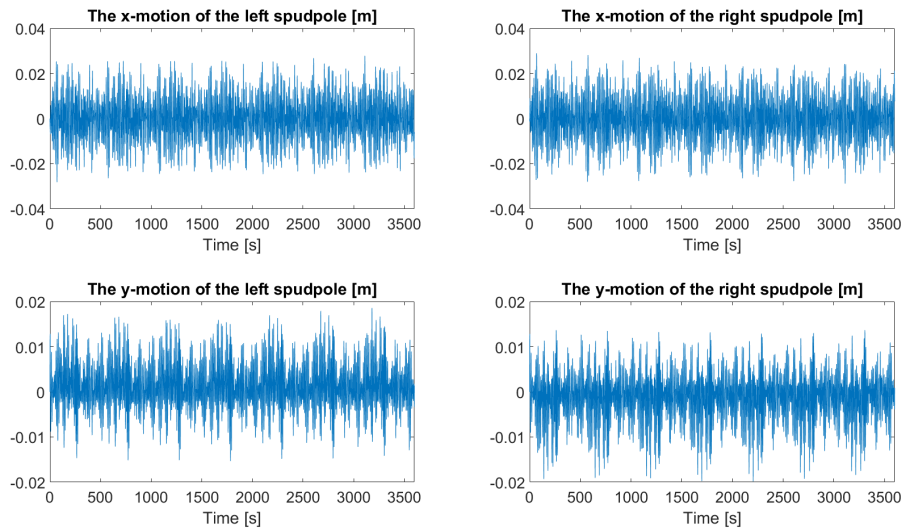


Figure D.1: The motions of the spudpoles in x and y direction ($D=8m, t=0.35m$, Wave direction 105°).

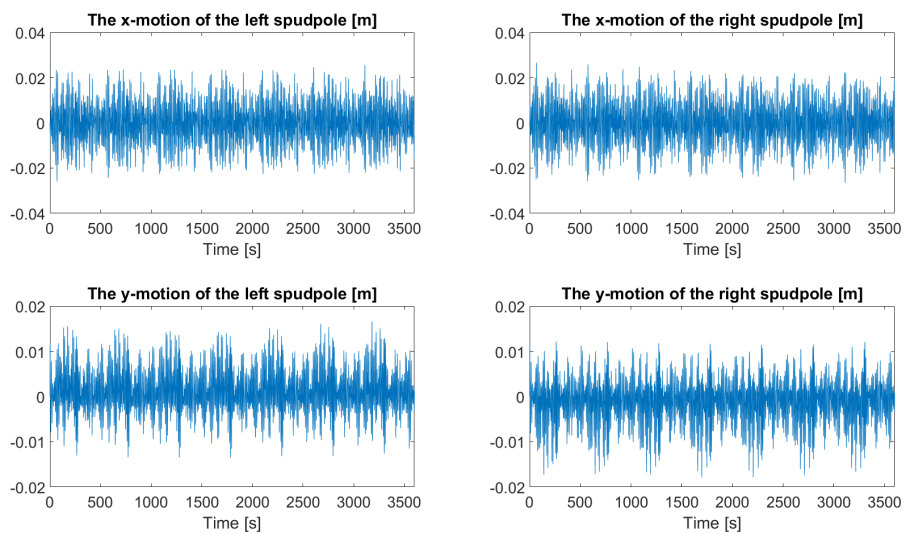


Figure D.2: The motions of the spudpoles in x and y direction ($D=8m, t=0.40m$, Wave direction 105°).

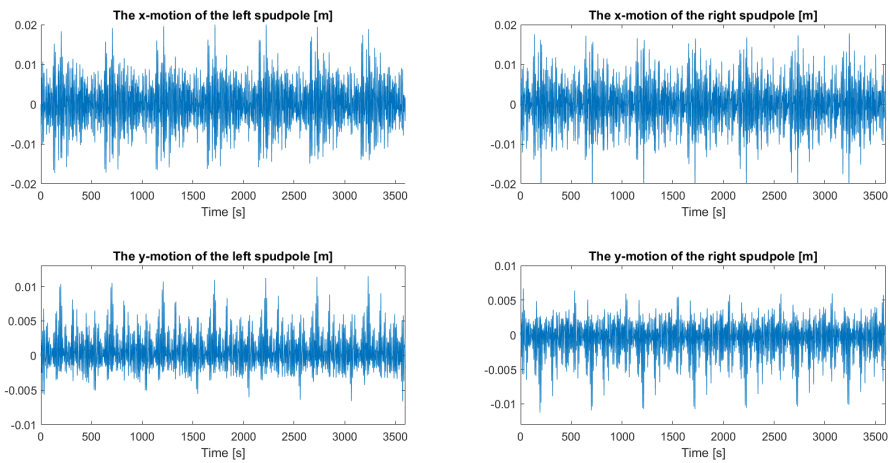


Figure D.3: The motions of the spudpoles in x and y direction ($D=8m, t=0.40m, \text{Wave direction } 135^\circ$).

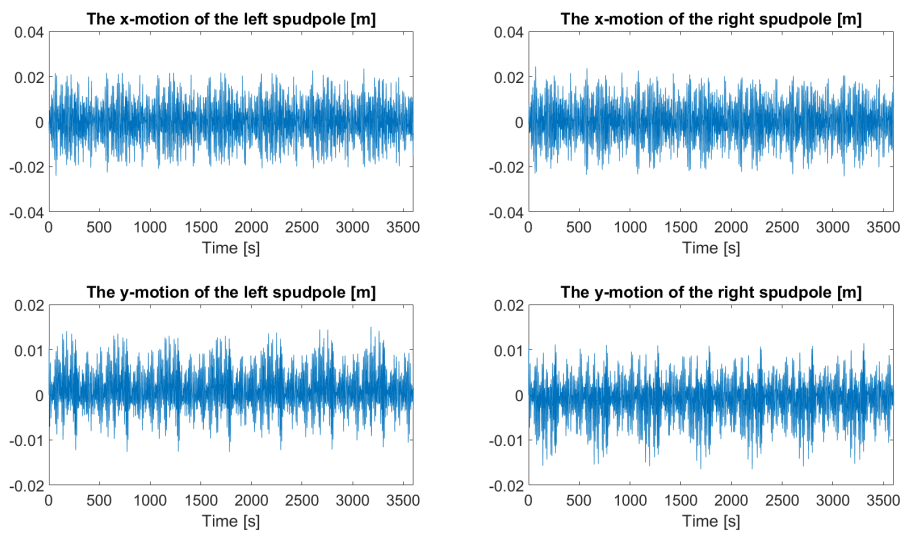


Figure D.4: The motions of the spudpoles in x and y direction ($D=9m, t=0.30m, \text{Wave direction } 105^\circ$).

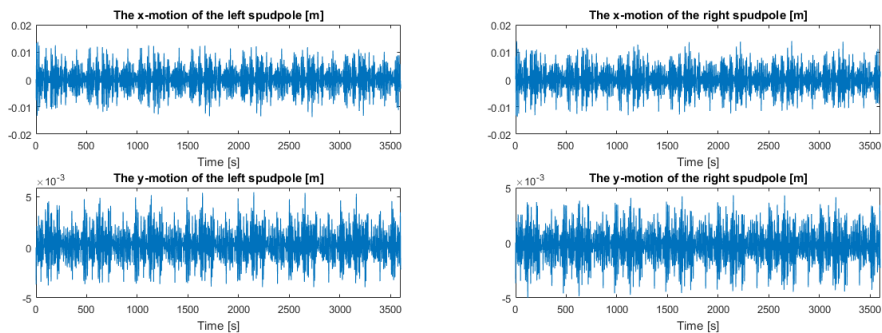


Figure D.5: The motions of the spudpoles in x and y direction ($D=9.5m, t=0.09m, \text{Wave direction } 105^\circ$).

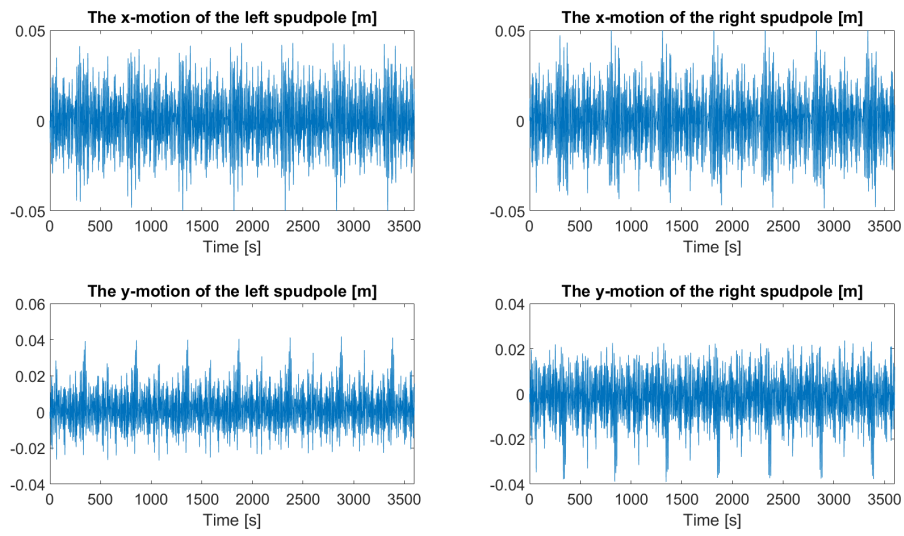


Figure D.6: The motions of the spudpoles in x and y direction ($D=10m, t=0.09m$, Wave direction 105°).

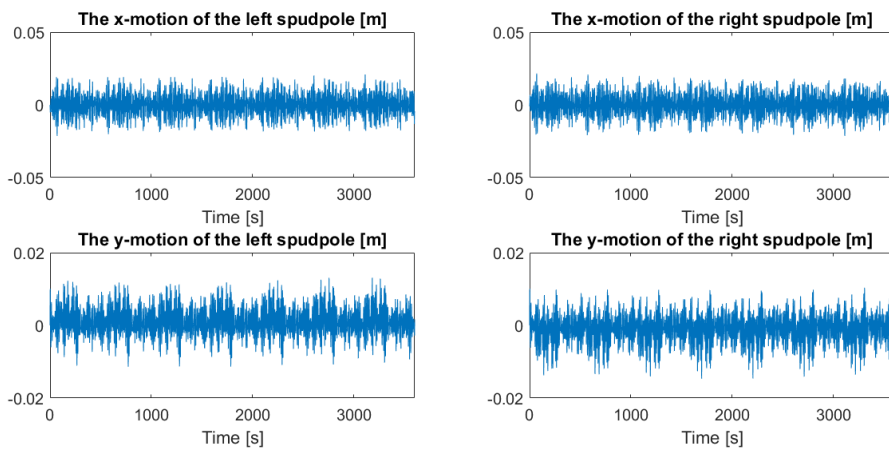


Figure D.7: The motions of the spudpoles in x and y direction ($D=10m, t=0.25m$, Wave direction 105°).

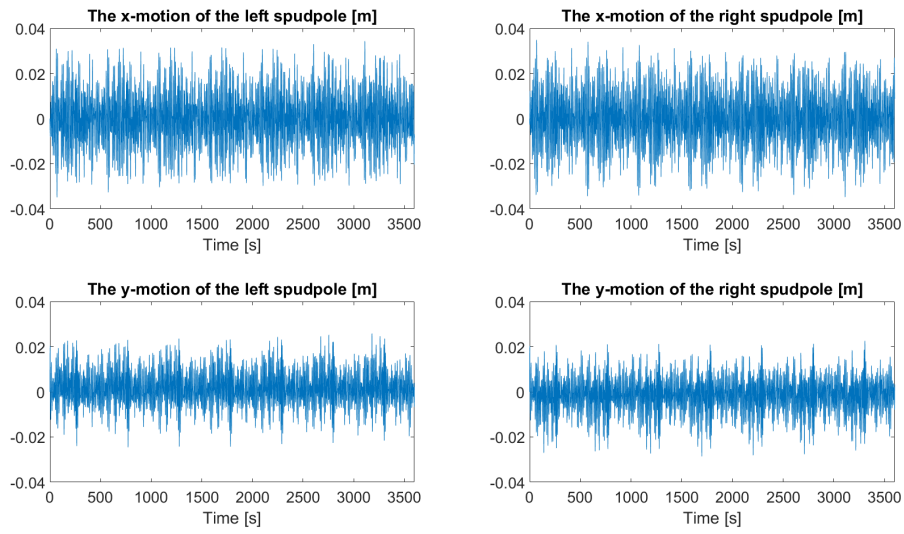


Figure D.8: The motions of the spudpoles in x and y direction ($D=11m, t=0.09m$, Wave direction 105°).

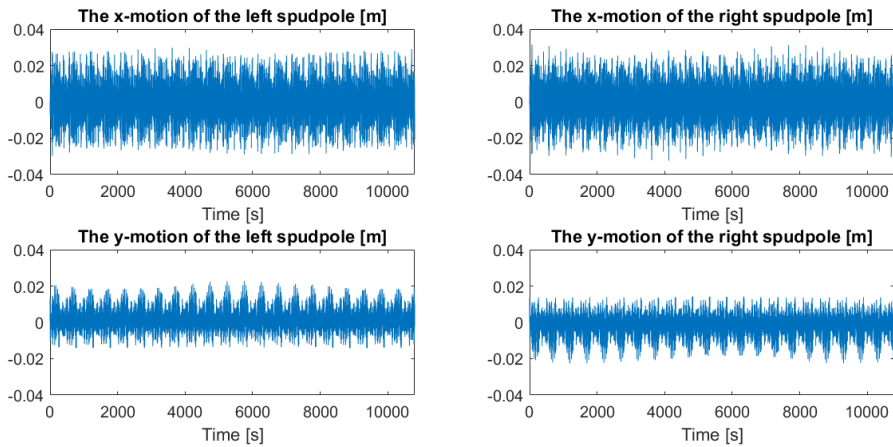


Figure D.9: The motions of the spudpoles in x and y direction ($D=11m, t=0.10m$, Wave direction 105°).

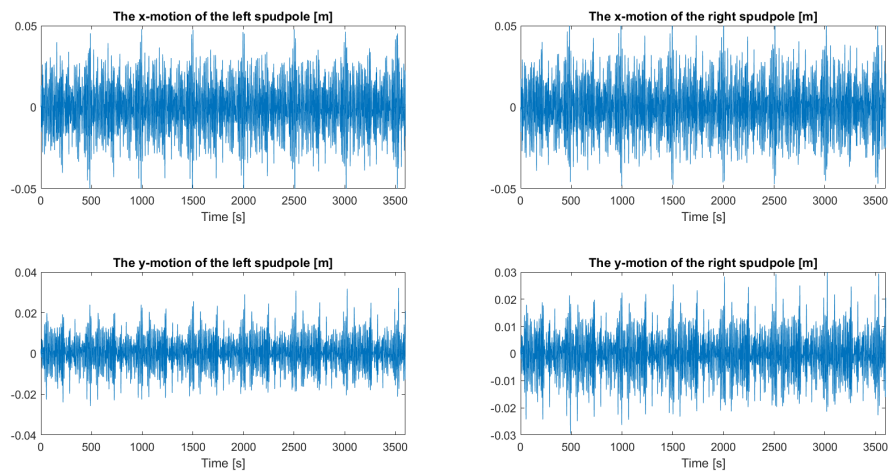


Figure D.10: The motions of the spudpoles in x and y direction ($D=11m, t=0.10m$, Wave direction 90°).